Quantum Dots-Converted Light-Emitting Diodes Packaging for Lighting and Display: Status and Perspectives

Bin Xie

State Key Laboratory of Coal Combustion and
Thermal Packaging Laboratory,
School of Energy and Power Engineering,
Huazhong University of Science and Technology,
Wuhan 430074, China

Run Hu

State Key Laboratory of Coal Combustion and
Thermal Packaging Laboratory,
School of Energy and Power Engineering,
Huazhong University of Science and Technology,
Wuhan 430074, China

Xiaobing Luo[1]

State Key Laboratory of Coal Combustion and
Thermal Packaging Laboratory,
School of Energy and Power Engineering,
Huazhong University of Science and Technology,
Wuhan 430074, China
e-mail: Luoxb@hust.edu.cn

Recent years, semiconductor quantum dots (QDs) have attracted tremendous attentions for their unique characteristics for solid-state lighting (SSL) and thin-film display applications. The pure and tunable spectra of QDs make it possible to simultaneously achieve excellent color-rendering properties and high luminous efficiency (LE) when combining colloidal QDs with light-emitting diodes (LEDs). Due to its solution-based synthetic route, QDs are impractical for fabrication of LED. QDs have to be incorporated into polymer matrix, and the mixture is dispensed into the LED mold or placed onto the LED to fabricate the QD–LEDs, which is known as the packaging process. In this process, the compatibility of QDs' surface ligands with the polymer matrix should be ensured, otherwise the poor compatibility can lead to agglomeration or surface damage of QDs. Besides, combination of QDs–polymer with LED chip is a key step that converts part of blue light into other wavelengths (WLs) of light, so as to generate white light in the end. Since QD-LEDs consist of three or more kinds of QDs, the spectra distribution should be optimized to achieve a high color-rendering ability. This requires both theoretical spectra optimization and experimental validation. In addition, to prolong the reliability and lifetime of QD-LEDs, QDs have to be protected from oxygen and moisture penetration. And the heat generation inside the package should be well controlled because high temperature results in QDs' thermal quenching, consequently deteriorates QD-LEDs' performance greatly. Overall, QD-LEDs' packaging and applications present the abovementioned technical challenges. A profound and comprehensive understanding of these problems enables the advancements of QD-LEDs' packaging processes and designs. In this review, we summarized the recent progress in the packaging of QD-LEDs. The wide applications of QD-LEDs in lighting and display were overviewed, followed by the challenges and the corresponding progresses for the QD-LEDs' packaging. This is a domain in which significant progress has been achieved in the last decade, and reporting on these advances will facilitate state-of-the-art QD-LEDs' packaging and application technologies. [DOI: 10.1115/1.4033143]

Keywords: quantum dots, light-emitting diode, packaging, color-rendering index

1 Introduction

Semiconductor QDs, as a promising material for absorbing and converting light energy, have attracted extensive scientific and industrial interests [1–3]. Since the emission and absorption characteristics of QDs are dependent on the particles' size, their band structures can be tuned according to the quantum confinement effect by varying the particles' size or compositions, as shown in Fig. 1. The elements in QDs are usually in group II–VI, such as CdSe [4]; group III–V, such as InP [5]; and group I–III–VI, such as $CuInS_2$ [6]. Due to their superior optical characteristics, QDs have been proven to be extremely suitable for many applications, such as optically or electrically pumped lasers, full color displays, LEDs, and biosensors [7–10]. Among these applications, QD-converted LEDs (QD-LEDs) are the most attractive application. There are two types of QD-LEDs, the differences are that one is based on photo-excited QDs (photoluminescence QD-LEDs), and another is electro-excited QDs (electroluminescence QD-LEDs). Here, we focus on the photoluminescence QD-LEDs, since they are the most commonly used type.

So far, the overall efficiency of electroluminescence QD-LEDs remained lower compared to that of photoluminescence QD-LEDs because of their charge injection problem. The conventional LEDs usually are phosphor-converted LEDs (pc-LEDs), which combine blue LED chips with yellow phosphors, e.g., yttrium aluminum garnet doped with cerium (YAG: Ce^{3+}) [11–13]. For pc-LEDs, the color-rendering index (CRI) is quite low owing to the lack of red component in the emission spectrum [14]. Moreover, the broad full-width-at-half-maximum (FWHM) of phosphors (50–100 nm) [15,16] makes it difficult to tune the spectra distribution of pc-LEDs, since it has significant overlap in the blue–green and green–red regions. In contrast, QD-LEDs have good CRI, wide absorption, and narrow emission spectra.

Quantum dots light-emitting diodes are usually used in thin-film display and general lighting applications, which is introduced in categories as follows:

(1) *Backlighting for Displays*: Color gamut is one of the most important parameters of display devices. This industry uses chromaticity diagrams and color gamut standards to quantify the color purity. The International Commission on Illumination (CIE) has established a chromaticity diagram known as CIE 1931 color space. Color gamut represents all colors that can be created by mixing primary colors. In 2013, Sony's commercial application of colloidal QD-based liquid crystal display (LCD) televisions used edge-
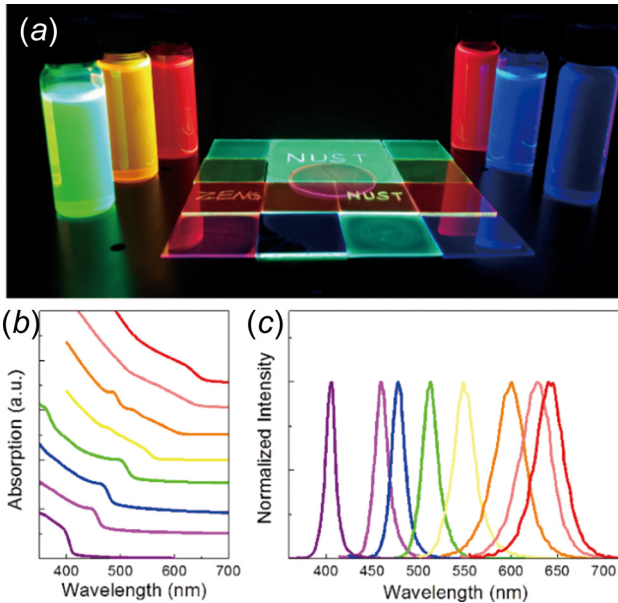
---

[1]Corresponding author.

Fig. 1 (*a*) Composition-dependent change of the emission color from colloidal solutions of all-inorganic perovskite cesium lead halide (CsPbX3, X = Cl, Br, I). (*b*) Optical absorption and (*c*) PL spectra of colloidal CsPbX3 QDs [17].

mounted red and green QDs to optically down-convert part of the blue LED backlight and reemitted red and green light. To achieve long-term luminescent stability, QDs were dispersed in an acrylate polymer and encapsulated in thin glass tubes to avoid oxygen and moisture exposure. The use of QDs for backlighting fulfills more than 100% of the National Television System Committee (NTSC) television color gamut standard [18]. Figure 2 shows the spectra
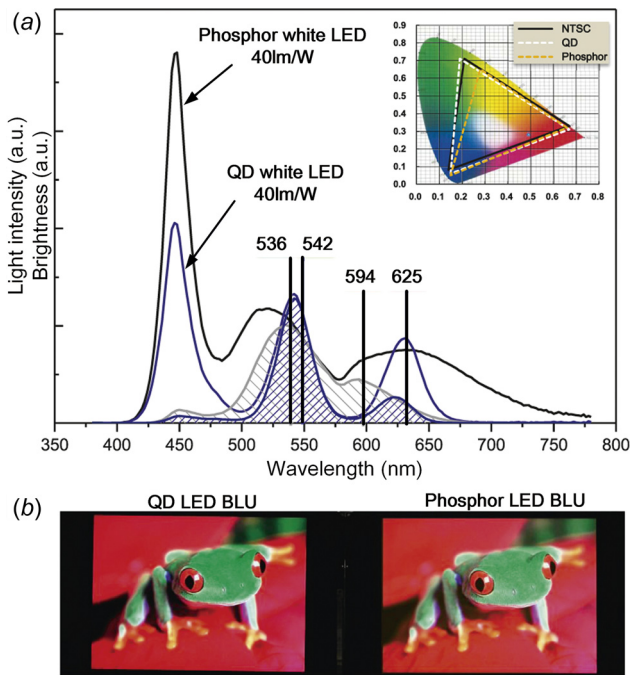

Fig. 2 (*a*) Light intensity spectra (solid line) and brightness (hatched area) of the QD-LED (blue) and the phosphor-LED (gray). Inset (*a*) indicates the color triangles created by the QD-LED (white) and the phosphor-converted LED (yellow). (*b*) Forty-six-inch LCD TV panel (Samsung displays) adapting QD-LEDs BLU (left) and phosphor LED BLU (right) [18] (See online for color).

distribution and photographs of a 46 in. QD-LEDs backlight unit (BLU) developed by Samsung displays. The QD-LED BLU (left of Fig. 2(*b*)) achieved 30% more NTSC color gamut than the conventional LED BLU (right of Fig. 2(*b*)). Furthermore, the color quality of QD-LCD is comparable to that of organic LED (OLED) displays while achieved at the cost of an LCD display. Thus, it represents an emerging technology and is expected to compete with OLED in the near future.

(2) *General Lighting*: As related to the human eyes, the correlated color temperature (CCT) and CRI are two major concerns of SSL. The CCT of a white light source is defined as the temperature of a planckian black-body radiator, whose color is closest to the color of the white light source. The CRI of a light source is defined as the ability of the light source to render the true colors of any objects (refer to Sec. 4.2 for details). The pc-LEDs produce "cold" white light with CCT > 5000 K and CRI < 85, which is not comfortable for human eyes. In order to realize a light source with warmer color and high CRI, red-emitting phosphors with narrow emission around 610 nm are added. But the development of efficient red phosphors still lags behind [19,20]. This challenge can be solved by narrow emission QDs. In 2009, QD Vision, Inc., had shown that by adding red-emitting QDs to the phosphor, it is possible to achieve white lighting with a CCT of 2700 K and a CRI > 90 while maintaining an efficiency of 65 lm/W [21]. Figure 3 shows the efficiency and CRI for different lighting applications; it is seen that the first commercial QD-LEDs have high CRI
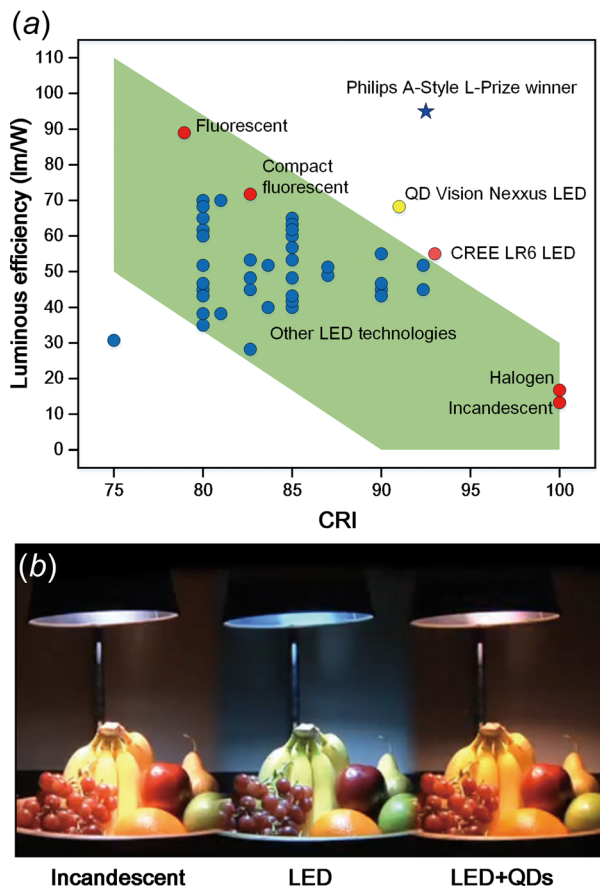

Fig. 3 (*a*) Efficiency and CRI for different lighting applications. The first commercial QDs-converted SSL solution developed by QD Vision and Nexxus Lighting has a high CRI while maintaining high LE. (*b*) Photographs comparing the illumination of objects with an incandescent lamp, a cool white LED, and the QD-LEDs. Photographs were quoted from QD Vision, Inc.

as well as high LE. In their technology, QDs in a transparent matrix are dispersed onto a substrate to form a QDs film with recorded solid-state QDs photoluminescence efficiency of 95% ± 5%. In 2008, Evident Technologies also developed their Christmas lights used blue LEDs to excite a mixture of CdSe/ZnS QDs dispersed in a polymer matrix to achieve monochromatic color emission across the visible spectrum, including colors such as purple and aqua that can typically only be achieved by color filtering of white light [22].

From above introductions, QD-LEDs are expected to create next-generation displays and high-quality lighting with better color gamut, higher efficiency, and high CRI. However, to quickly penetrate the applications, many packaging issues of the QD-LEDs should be solved. QDs have to be incorporated into polymer matrix, and the resulting QDs mixture is dispensed into the LED mold or placed onto the LED in terms of QDs–polymer film, which is known as the packaging process. Packaging is an essential step, which not only can ensure better performance of LED devices by enhancing reliability and optical characteristics but can also realize control and adjustment of the working performance. Therefore, the packaging process needs to be deeply studied to achieve high-quality QD-LEDs devices, which is the right motivation behind this review. Here, the basic knowledge of QD-LEDs in lighting and display was introduced, followed by the discussion on the challenges and the corresponding progresses for the QD-LEDs packaging.

2 Brief Knowledge of QD-LEDs Packaging

Figure 4 shows the packaging process of QD-LEDs. Typically there are two types of packaging structure of QD-LEDs, one is the remote type and another is the on-chip type. Taking the remote type as an example, step by step, the packaging processes are as follows:

(a) *QDs Mixed With Polymer Matrix:* The solution-based QDs are blended with polymeric matrix which can be processed or manipulated into the solid-state material, and then the

mixture is stirred to obtain homogeneous QDs–polymer hybrid material. In this process, the compatibility of QDs' surface ligands with the polymer should be ensured. Otherwise the poor compatibility can lead to agglomeration or surface damage of QDs.

(b) *Solidification of QDs–Polymer Mixture*: Firstly, the organic solvent in the QDs–polymer mixture is moved in the vacuum chamber, and then the mixture is fabricated into solid film or stick. According to the characteristic of polymer matrix, solidification can be achieved by different methods, such as electrochemical reactions [23–25], utilization of gamma and ultraviolet (UV)-irradiation [26–28], and thermal curing reactions [29–31].

(c) *Combination of QDs–Polymer With LED Chip*: The QDs–polymer composite is fabricated onto LED chip with blue emission, and QDs convert part of the blue light into other expected WLs, resulting in white light after color mixing. The optical efficiency as well as the thermal performance of QD-LEDs are dependent on the packaging structure. Besides, the color-rendering quality is determined by the color mixing process. Therefore, packaging structure needs to be well controlled to achieve high light output and better heat dissipation performance, and the color mixing of different QDs particle should be optimized for higher color-rendering quality.

(d) *Encapsulation*: The encapsulant is filled into the interspace between the QDs–polymer film and LED chip to protect the chip and bonding wires. The QDs are also protected by encapsulant to avoid direct contact with oxygen and moisture. The encapsulant coating can improve the long-term stability and its morphology can also influence the light output efficiency.

The packaging process of the on-chip type QD-LEDs is quite similar with the remote type. Firstly, the QDs are mixed with polymer matrix (a). Then the QDs–polymer mixture is coating onto the LED chip (b2). After the solidification of QDs–polymer mixture (c2), the whole QDs–polymer gel is covered by encapsulant (d2) to protect the chip and QDs.

3 Challenges in QD-LEDs' Packaging

From the packaging processes shown in Fig. 4, there are several key problems in QD-LEDs' packaging and applications.

3.1 Compatibility Problem of QDs and Polymers. Due to the solution-based synthetic route in which QDs are suspended in some organic solvent, QDs are impractical for fabrication and integration of light-emitting devices directly. So the solidification of well-defined QDs–polymer hybrid materials is prerequisite before applications. However, hydrophobic surface of typical QDs is generally incompatible with the conventional LED packaging process, where the QDs are physically blended with silicone or epoxy resin. The hydrophobic organic ligands on QDs' surface damage the polymerization of resin encapsulation, namely, the catalyst poisoning effect [32]. Besides, the incompatibility of QDs' surface with polymer matrix can result in QDs agglomeration, consequently decrease the photoluminescence efficiency of QDs [33–35].

3.2 Combination of QDs With LEDs. Combination of QDs–polymer with LED chip, as shown in Fig. 4(c), is the key component that converts part of blue light into other WLs of light. QD-LEDs always consist of three or more kinds of QDs. Therefore, the spectra distribution should be optimized, through tuning the WLs and mixing ratio of QDs components, to achieve a high color-rendering ability. This requires both theoretical spectra optimization and experimental validation. In addition, the packaging structure plays an important role in determining the final optical characteristics of QD-LEDs. Improper QDs–polymer morphology
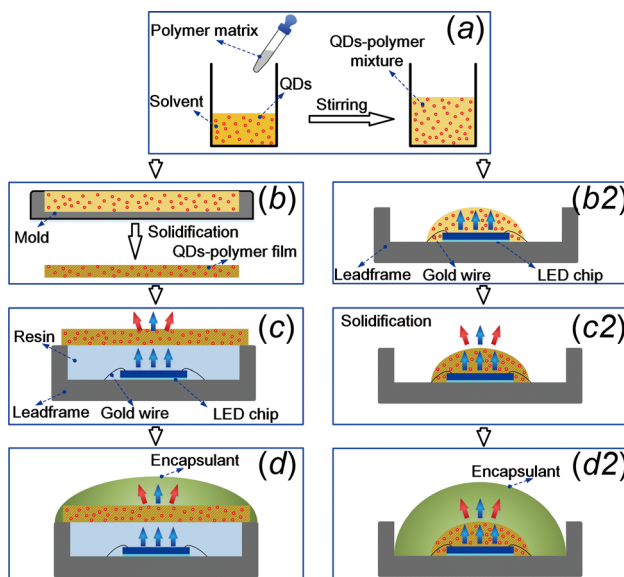
Fig. 4 Typical packaging process of QD-LEDs: (*a*)–(*b*)–(*c*)–(*d*) are the packaging steps for remote type QD-LEDs and (*a*)-(*b*2)-(*c*2)-(*d*2) are the packaging steps for on-chip type QD-LEDs. (*a*) QDs mixed with polymer matrix, (*b*) solidification of QDs–polymer mixture, (*c*) combination of QDs–polymer with LED chip, and (*d*) encapsulation; (*b*2) coating of QDs–polymer mixture, (*c*2) solidification of QDs–polymer mixture, and (*d*2) encapsulation.

and QDs particle distribution may cause low efficiency or poor color quality. The packaging structure should be well designed in this process.

3.3 Reliability and Lifetime of QD-LEDs. To prolong the reliability and lifetime of QD-LEDs, the QDs have to be protected from oxygen and moisture. Besides, the heat generation from QDs should be well controlled because high temperature results in QDs' thermal quenching, consequently deteriorates QD-LEDs' performance greatly.

In the last decade, most of the progresses in QD-LEDs' packaging are aiming to solve aforementioned problems, which will be reviewed as follows.

4 Progresses in QD-LEDs' Packaging and Applications

4.1 Compatibility of QDs and Polymer Matrix. Before the applications of white LED (WLED), issues about the poor compatibility of QDs with polymeric environments should be resolved. Although techniques for incorporating QDs in thin films are well developed, stabilizing these QDs in bulk polymer matrices remains a challenge. The approaches are mainly focused on the preparation of well-dispersed QDs inside polymers so that the photoluminescence properties of QDs are not affected [36,37]. In addition, the QDs–polymer composites are required to be transparent when encapsulated into the LEDs. Therefore, it is required to establish methods to obtain QDs–polymer materials with high transparency and uniformity.

4.1.1 Modification of the QDs' Surface Chemistry. The main strategy to improve the compatibility and dispersibility of the QDs and polymer is to coat compatible ligands at the surface of the QDs. For example, coating CdS QDs with ligands
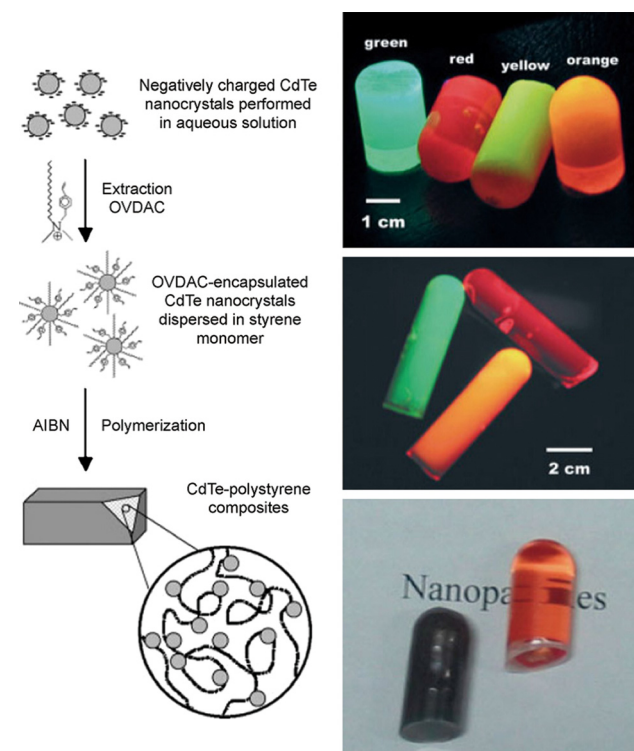

Fig. 5 CdTe/polystyrene hybrid materials using a polymerizable surfactant. Aqueous CdTe QDs were preprepared, and polymerizable OVDAC was used as a surfactant to transfer negatively charged CdTe QDs to a styrene solution. After radical polymerization, a transparent CdTe-PS composite was obtained [41].

functionalized by phenyl groups improved the dispersibility of the QDs in pyridine [38], and oleic acid ligands at the QDs surface promoted the solubility of the QDs in polymethylmethacrylate (PMMA) and PS, while an octylamine at the QDs' surface results in a strong quenching of band-edge emission [39].

By introducing covalent bonds, such as 4-thiomethylstyrene as both a capping ligand and a comonomer to replace the trioctyl-phosphine oxide (TOPO) on CdSe, QDs–polystyrene composites were successfully obtained after polymerization [40]. Ligands modification can be realized by the direct modification of the periphery with surfactants, which is able to copolymerize with the growing polymer chains. Zhang and coworkers [41] have demonstrated a method by using octadecyl-*p*-vinyl-benzyldimethylammonium chloride (OVDAC) as a polymerizable surfactant to transfer the aqueous CdTe QDs into styrene or methyl methacrylate monomer solutions, a transparent CdTe–PS composite was obtained. Figure 5 shows these CdTe/polystyrene hybrid materials.

4.1.2 Incorporation of QDs Into Polymer Materials. The QDs can be encapsulated by an optically transparent barrier material to minimize the incompatibility problem. For instance, QDs–silica composite including silica shell overcoating individual QDs [42–44], multiple QDs-embedding silica matrix [45–46], and QDs–silica monolith [47,48] were obtained in terms of powder-typed QDs–silica composites by the microemulsion method. Since the surface of QDs is coated with silica layer, catalyst poisoning does not occur during the curing process of the silicone [45]. Compared to the QDs–WLED with bare QDs, the silica-embedded CIS/ZnS QDs showed a longer operational times (1–3 h), but a lower blue-to-yellow conversion efficiency due to the PL reduction concomitant to silica-embedding procedure [49].

Instead of the modification of surface ligands of nanocrystals, electrostatic interaction between negatively charged QDs and a positively charged building block can be the main driving force to achieve the desired hybrid QDs–polymer material [50–52]. The QDs act as physical cross-linking centers, and the resulting complexes are easily shaped into various fluorescent structures and materials, the stability of the photoluminescence properties was improved as well. Tetsuka et al. [53] demonstrated a method of incorporating the hydrophilic CdSe/ZnS QDs into a transparent and flexible clay host, which was realized through electrostatic interaction between QDs' surface and clay platelets. Similarly, Qi
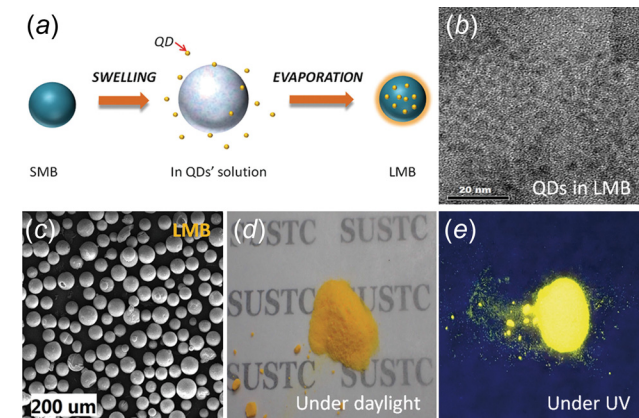
Fig. 6 (*a*) Schematic of incorporation of QDs into a silica bean by the swelling and solvent-evaporation method. The silica microbeans solution were preheated at 60 °C, whereby the pores in the silica increase in size allowing the QDs with their outer organic ligands to enter into the mesoporous structure. The final LMBs powders were obtained after drying process. (*b*) Transmission electron microscope image of QDs in LMBs, (*c*) Scanning electron microscope (SEM) image of LMBs, (*d*) photograph of as-prepared LMBs under daylight, and (*e*) photograph of LMBs under UV light (365 nm) [56].

et al. [54] proposed a method combining the electrostatic modification of CdTe QDs and the titania sol–gel process to fabricate stable QDs/TiO₂ hybrid film. The CdTe QDs were wrapped in a cationic surfactant and a surfactant-encapsulated QDs hybrid particle with hydroxyl active sites on its periphery was formed. Due to this structure in which QDs' surface was better passivated by the polymer, the original luminescent property of QDs and the flexibility of titania sol–gel materials were retained in the resulting hybrid films.

4.1.3 Embedding QDs Into Polymer Microspheres. Another effective way to improve the dispersibility and stability of QDs inside the polymers is to embed QDs into the microspheres. Swelling is the simplest method for preparing QDs–polymer microspheres. The swelling polymers trap the QDs inside the particle, and the subsequent washing of the residue causes the polymer to shrink, thus trapping the QDs inside the microspheres [55]. Chen et al. [56] obtained luminescent microbeans (LMBs) by a swelling method which combines mesoporous silica particles with the CuInS₂ (CIS) QDs. Figure 6(a) shows the schematic diagram of this swelling and solvent-evaporation method; Figs. 6(b)–6(d) show the images of the as-prepared LMBs. The mesoporous structures work as the lattice to avoid aggregation of the QDs.

The swelling method results in as many as 10^3–10^5 nanoparticles embedded into polymer microspheres, while there is no Förster energy transfer between the QDs, which indicates that the embedded QDs are well dispersed without aggregation [55,57]. Furthermore, due to the restrict of the mesoporous, only QDs within a certain size range can be incorporated, thus narrowing the QDs size distribution, and consequently narrowing the emission spectra of the hybrid microspheres. The main concern of this method is that the QDs' penetration is highly dependent on the swelling conditions and the degree of cross-linking. The QDs only penetrated into the edge of the microspheres in the condition of low degrees of swelling or high cross-linking densities, as revealed by Bradley et al. [58].

4.2 Spectra Optimization of QD-LEDs. To generate high-quality white light, which is suitable for lighting and display applications, it is important to design the spectrum distribution of QD-LEDs. Before covering the researches of spectra optimization, we first introduce several concepts of color science:

(1) *Color Matching Functions and Chromaticity Diagram*: Since light causes different levels of excitation of red, green, and blue cones, the sensation of color and luminous flux of a particular color varies slightly among different individuals. Furthermore, the sensation of color is a subjective quality that cannot be measured objectively. Therefore,
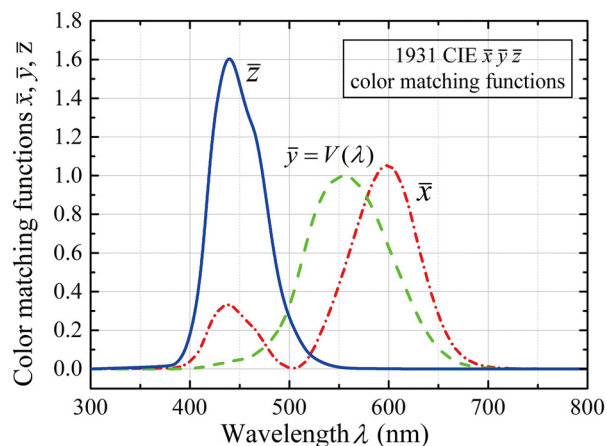
the CIE has standardized the measurement of color using color matching functions and the chromaticity diagram. Figure 7 shows the CIE color matching functions. The three color matching functions $x(\lambda)$, $y(\lambda)$, and $z(\lambda)$ approximately correspond to the eye sensitivity curves of the red, green, and blue cones, respectively.

The perception of colored light can be analyzed in terms of the degree to which the light stimulates the three types of cones. The degree of stimulation of the three types of cones is given by

$$X = \int_\lambda \bar{x}(\lambda)P(\lambda)d\lambda \tag{1}$$

$$Y = \int_\lambda \bar{y}(\lambda)P(\lambda)d\lambda \tag{2}$$

$$Z = \int_\lambda \bar{z}(\lambda)P(\lambda)d\lambda \tag{3}$$

where $P(\lambda)$ is the spectral power distribution, and X, Y, and Z are the tristimulus values that indicate the relative stimulation of each of the three cones. The chromaticity coordinates x and y are calculated from the tristimulus values according to

$$x = \frac{X}{X+Y+Z} \tag{4}$$

$$y = \frac{Y}{X+Y+Z} \tag{5}$$

$$z = \frac{Z}{X+Y+Z} = 1 - x - y \tag{6}$$

Figure 8 shows the chromaticity diagram, which is created by using the mapping methodology described in Eqs. (1)–(6). Monochromatic or pure colors are found on the perimeter of the chromaticity diagram. White light is found in the center of the chromaticity diagram.

(2) *Color Gamut*: In LED displays, three different types of LEDs, usually emitting in the red, green, and blue are used. The three colors are mixed so that the observer sees a

Fig. 7 CIE (1931) color matching functions. The y(λ) color matching function is identical to the eye sensitivity function V(λ) (See online for color).
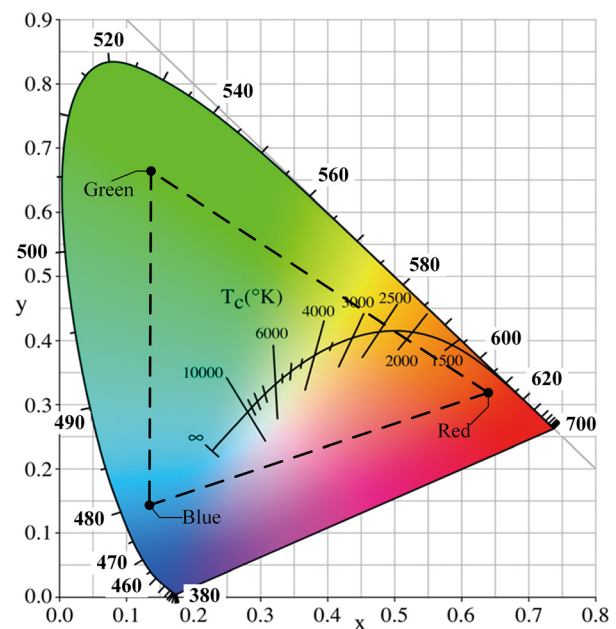
Fig. 8 CIE 1931 (x, y) chromaticity diagram. The triangular region referred to as the color gamut created by three primary colors (See online for color).

mixture of the three colors. White LEDs also emit two or three complementary colors. Figure 8 shows the CIE 1931 chromaticity diagram and the schematic diagram of color gamut created by three primary colors. The color gamut represents all colors that can be created by mixing primary colors, e.g., red, green, and blue.

(3) *CRI and Color Quality Scale (CQS)*: CRI is a measure of the ability of an illuminant, i.e., an illumination source to render all the colors of an object illuminated with the light source. The color-rendering ability of a test light source is evaluated by comparing it with a reference light source. The reference light source for calculation of the CRI is a planckian black-body radiator with the same color temperature or CCT as the test light source. The reference light source has ideal color-rendering properties and its CRI is 100. Illuminants other than the chosen reference light source have a CRI lower than 100.

The 1976 CIE general CRI is calculated according to

$$\text{CRI}_{\text{general}} = \frac{1}{8}\sum_{i=1}^{8}\text{CRI}_i \qquad (7)$$

where the CRI_i are the special color-rendering indices for eight sample objects. The special CRI are given by

$$\text{CRI}_i = 100 - 4.6\Delta E_i^* \qquad (8)$$

where ΔE_i^* is the difference in color that occurs when a sample object is illuminated with the reference illumination source and the test illumination source. Further information regarding these color renditions can be found in Ref. [59]. Besides, there is another index to evaluate the color-rendering capability of the illuminants, the CQS, which was developed by Davis and Ohno [60]. It uses the same reference light sources as in the CRI, but the test color samples are changed. The CQS uses 15 reflective Munsell samples and it makes use of a saturation factor. In addition, the CQS ranges from 0 to 100, which is more understandable because $\text{CRI} < 0$ does not express any useful information. The advantage of the CQS is that it provides a better scale and understanding for the color-rendering capability of the LED spectra.

(4) *Luminous Efficacy of Optical Radiation (LER) and LE*: The efficiency of the white light sources needs to be evaluated by considering the eye sensitivity function. There are two important efficient criteria used for this purpose. The first is called the LER. It is calculated according to

$$\text{LER} = \frac{683\frac{lm}{W_{\text{opt}}}\int P(\lambda)V(\lambda)d\lambda}{\int P(\lambda)d\lambda}\, lm/W_{\text{opt}} \qquad (9)$$

where W_{opt} and $V(\lambda)$ are the optical power and photopic eye sensitivity function, respectively. A white light spectrum having an LER as high as possible is desirable as it means more optical energy is radiated at the WLs where the eye is sensitive. The second important criterion is called the LE, calculated by Eq. (10). The LE calculates the LER with respect to the supplied electrical power, P_{elect}:

$$\text{LE} = \text{LER} \times \frac{\int P(\lambda)d\lambda}{P_{\text{elect}}}\, lm/W_{\text{ele}} \qquad (10)$$

Based on the brief introduction of these important evaluation indices for light-emitting devices, we consequently summarize the studies referring to the spectral design of QD-LEDs for lighting and display applications. Since each application has different requirements and some applications have complicated tradeoffs between the performances' criteria, the optimization of the white light spectrum is a complicated task.

4.2.1 Photometric Optimizations for Lighting Applications. In order to obtain a well-designed QD-LEDs suitable for lighting applications, criteria such as CRI and LER have to be simultaneously considered when designing the spectrum, i.e., there are tradeoffs between CRI and LER. A photometric study of QD-LEDs exhibiting high CRI and LER is reported [61]. Various spectral designs have been simulated to understand the correlations between these two parameters. It is concluded that the maximum obtainable CRI decreases as the LER increases, and a warm-white LEDs with CRI > 90 and LER > 380 lm/W at a CCT of 3000 K can be achieved theoretically. The relation between CRI and LER is reasonable, because if one source has a high CRI, its spectrum should have a power distribution covering the visible region, while LER decreases with wider emission spectrum.

Besides, to achieve QD-LEDs with high optical performance, the FWHM, peak emission WL, and the relative amplitude of each QDs color component need to be designed. According to the results from previous studies [61,62], four colors in blue, green, yellow, and red spectral ranges are recommended in the packaging of WLED. The optimal peak WLs are 465 nm for blue, 527 nm for green, 569 nm for yellow, and 620 nm for red, and the corresponding FWHMs should be 44 nm, 43 nm, 44 nm, and 32 nm,

Table 1 Optimal spectral parameters of QD-LEDs leading to the highest LERs satisfying CRI = 95 and R9 = 95 at 1500 K ≤ CCT ≤ 6500 K [63]

| CCT (K)	2700	3000	3500	4000	4500	5000	5700	6500
Blue WL	462.5	462.3	461.6	460.9	460.2	461.1	460.4	459.7
Green WL	520.9	521.6	522.4	522.9	523.3	523.7	523.9	523.9
Yellow WL	566	566	566.2	566.6	567	566.7	567.4	568.2
Red WL	623.7	623	622.1	621.5	621	620.7	620.4	620.1
Blue FWHM	30	30	30	30	30	30	30	30
Green FWHM	30	30	30	30	30	30	30	30
Yellow FWHM	30	30	30	30	30	30	30	30
Red FWHM	30	30	30	30	30	30	30	30
Blue amplitude (%)	7.82	10.67	15.13	19	22.37	24.77	28.22	31.31
Green amplitude (%)	15.72	17.65	20.24	22.2	23.63	25	25.99	26.67
Yellow amplitude (%)	27.1	26.57	25.18	23.64	22.17	20.82	19.4	18.12
Red amplitude (%)	49.36	45.11	39.46	35.16	31.83	29.42	26.4	23.9
CRI	95	95	95	95	95	95	95	95
R9	95	95	95	95	95	95	95	95
CQS	93	94	94	93	93	93	93	93
LER (lm/W_{opt})	370	371	367	360	352	347	338	327
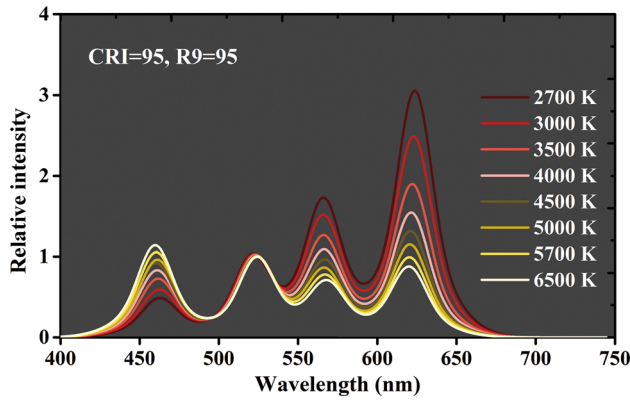
Fig. 9 Optimal spectra of QD-LEDs leading to the highest LERs satisfying CRI = 95 and R9 = 95 at 1500 K ≤ CCT ≤ 6500 K [63]

respectively [61]. It is worth noting that the above results were concluded without considering the rendering of test color sample 9 (R9) for the strong red. Zhong et al. obtained the optimized peak WL and FWHM of each color component for maximizing the LER of QD-LEDs under conditions of both CRI and R9 above 95. Table 1 lists the optimal spectral parameters, and Fig. 9 plots the corresponding spectra [63].

Although the optimal spectra of QD-LEDs can be obtained by spectra optimization algorithm, reproducing these spectra in laboratory is not that easy, because there is less literature referring to the optical modeling of QD-LEDs. At the very beginning, the optical performance of QD-LEDs is limited [64–66]. In 2007, Demir et al. demonstrated QD-LEDs based on cyan, green, orange, and red CdSe/ZnS QDs, which achieved relative low CRI of 71 [66]. Three years later, the researchers enhanced the performance of their device using the same material system [67]. By using green (528 nm), yellow (560 nm), and red (609 nm) CdSe/ZnS QDs, this QD-LEDs achieved a LER of 357 lm/W_{opt} along with a CRI of 89.2 and a CCT of 2982 K. In recent years, research efforts began to focus on increasing the optical performance of QD-LEDs based on cadmium-free QDs, such as CuInS QDs [68,69] and InP QDs [70,71]. After optimization, a white QD-LEDs using InP/ZnS core–shell QDs achieved a CRI of 89.3 and an LER of 254 lm/W_{opt} at a CCT of 2982 K [72].

At the end of this part, we concluded other experimental studies referring to the spectra optimization of QD-LEDs for general lighting. Figure 10 shows a summary of CCT, LE, and CRI of the experimentally achieved QD-LEDs [73–98]. It is seen from the figure that there is still room to improve the optical performance of QD-LEDs for general lighting applications. To reach its highest point of overall performance, more collaborative works combining optical simulation with experimental validation have to be done in the near future.
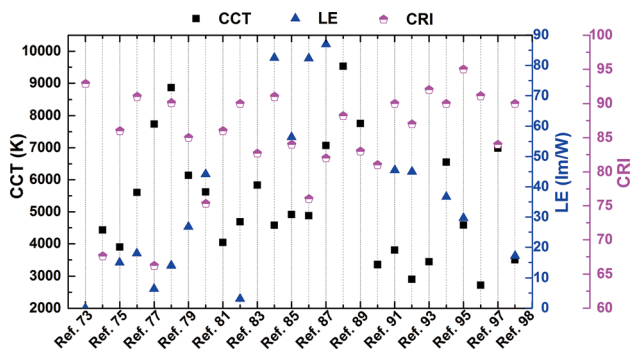

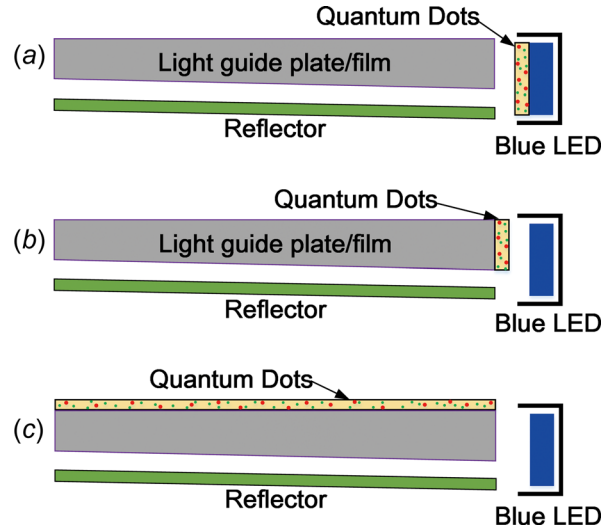**Fig. 10** Performance collection of QD-LEDs sorted according to years [73–98]

Fig. 11 Schematic diagram of three different packaging structures of QDs-incorporated BLU: (*a*) on-chip, where the QDs are placed within the LED package which is coupled to the light guide plate, (*b*) on-edge, where the QDs are placed in between the LED package and the light guide plate, and (*c*) on-surface, where the QDs are in a thin film over the entire display area

4.2.2 Colorimetric Optimizations for Display Applications. In comparison to lighting applications, backlight products utilizing QDs as down-convertors have already begun to find commercial applications. In 2013, Sony, in cooperation with QD Vision, launched the world's first QDs television using Color IQ optics [99]. Nanosys and 3M have demonstrated the similar strategies using their quantum dot enhancement film (QDEF) [100]. By adding QDEF, the display maker can immediately begin to produce LCD panels with color and efficiency performance beyond OLEDs, without making any changes to established processes.

Figure 11 shows the schematic diagram of three typical packaging structures to incorporate QDs into BLU, i.e., on-chip, on-edge, and on-surface types [101]. The on-chip type can be a direct replacement of the phosphor-based BLU, while the on-edge and on-surface types belong to the remote type, which can protect QDs from the thermal effect caused by the LED chip. In addition, the on-edge type does not change the configuration of optical stacks inside the LCD, while the on-surface type usually incorporates QDs with other optical films such as prism sheet. Besides, the amount of material needed for the on-surface type and on-edge type scales with display sizes. The on-surface type consumes a lot more QDs materials than the on-edge one. Therefore, the on-surface type is more favorable to small panels while the on-edge type is more attractive to large panels.

Figure 12 plots a typical edge-lit LCD system with on-surface QDs structure. It contains a blue LED source, light guide plate to guide the light source toward the thin film transistor–LCD panel, QDs film, a series of optical stacks, and polarizers. Different from the spectra optimization of QD-LEDs for lighting applications,
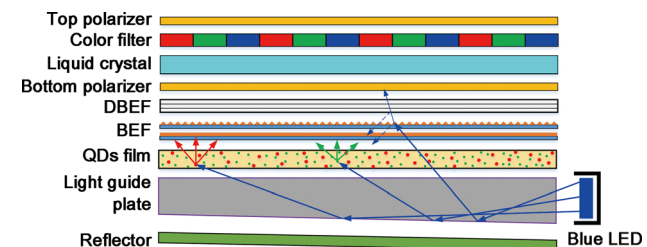

Fig. 12 A typical edge-lit LCD system with on-surface QDs structure

when designing the spectra distribution of backlighting, we expect to obtain a wider color gamut and higher total light efficiency (TLE), which is defined as

$$\text{TLE} = \frac{683 \frac{\text{lm}}{W_{\text{opt}}} \int S_{\text{out}}(\lambda)V(\lambda)d\lambda}{\int S_{\text{in}}(\lambda)d\lambda} \qquad (11)$$

where $S_{\text{out}}(\lambda)$ and $S_{\text{in}}(\lambda)$ are the output and incident spectra power density of the BLU, respectively. Demir et al. concluded that in order to cover 100% NTSC color gamut, the FWHM of the QDs should be at most 50 nm. Otherwise the green end of the NTSC triangle cannot be included. Additionally, the blue emission should be generated with a source having an FWHM no more than 70 nm [102].

To simultaneously achieve a large color gamut and high TLE, we have to consider the effect of optical stacks inside LCD on the output light spectra. Among these optical stacks, the liquid crystal is used to modulate the input light, and the color filter is used to select the red, green, and blue colors according to a specific

Fig. 13 (*a*) Transmission spectra of three commercial color filters. CF1 has the highest transmission peak but it has significant overlap in the blue–green and red–green regions. CF2 and CF3 employ green photoresist with a narrower FWHM but their transmittance is sacrificed. (*b*) The optimal performance of QDs backlight for different CFs. (*c*) The optimal performance of QDs backlight with different FWHM lower limits [104] (See online for color).

transmission characteristics. Therefore, besides the input light spectra, the color of the LCD can be affected by the transmittance of the color filter and the WL dispersion of the liquid crystal material. Although the overall transmittance of different modes of liquid crystal slightly depends on the WL, the shape of these transmission curves remains quite similar [103]. Therefore, the color filter plays the major role in terms of reshaping the output light spectra. Figure 13 shows the transmission spectra of three commercial color filters and the optimal performance of QDs backlight for different CFs [104]. Wu and coworkers [105] demonstrated that narrow band color filters are not effective for QDs backlight, especially when considering the loss in light efficiency. This is attributed to the pure emission peaks of QDs backlight, which is less dependent on the color filters [104]. Therefore, the cost can be reduced and the optical efficiency can be further improved by using broadband color filters. In addition, the FWHM of QDs emission can affect the display performance. As shown in Fig. 13(*c*), as the lower limit of green QDs ($\Delta\lambda_g$) and red QDs ($\Delta\lambda_r$) increases from 10 nm to 50 nm, both color gamut and TLE are reduced [104]. This is reasonable since a broader emission band results in less saturated color primary and decreases the transmittance toward color filter. Therefore, narrower QDs emission is preferred for a high-performance BLU. Recently, metal halides perovskite QDs [106,107] show very narrow FWHM of ~10 nm. This material can further improve the display performance of QDs backlight.

4.3 Enhancing the Reliability and Lifetime of QD-LEDs. In order to enhance the reliability and lifetime of QD-LEDs, we have to consider two primary reasons that will lead to the optical performance degradation of QD-LEDs. One is QDs' PL degradation caused by oxygen and moisture penetration [108]. The penetrative oxygen and moisture could corrode the surface ions and ligands of QDs, consequently resulting in defect trap states that cannot be ignored [109–111]. To suppress this defect, two solutions were proposed in previous studies, one is to coat the nanocrystals with extra ligands, and another is to create a barrier layer on the outer surface of polymer film.

Another primary reason for the degradation of QD-LEDs is the QDs thermal quenching effect [112]. The quenching mechanism involves nonradiative relaxation of conduction band electrons through the thermally created temporary trap states [113]. To solve this problem, packaging structure has to be optimized for better thermal stability. It is worth noting that we mainly discuss the thermal management inside of the package and that outside of the package is not included in this section. This is because of the similarity in the outer packaging structure between QD-LEDs and pc-LEDs, and solutions for heat dissipation from the package to the ambient are widely studied in previous works [114–117].

4.3.1 Improving Stability of QDs Against Oxygen and Moisture. The oxygen transmission rate (OTR) and the water vapor transmission rate (WVTR) are the evaluation indices of the gas resistance capability of the material. Since penetrative micro-molecules are able to diffuse across the polymer coating layer and causing chemical oxidation of atoms on the QDs' surface, an extra surface coating on the QDs' surface can act as the buffer layer to react with the micromolecules before it can react with the QDs, consequently lower the OTR and WVTR. For instance, coating surface ligands having free amines, such as mercaptoethanol, can protect QDs from oxidative quenching by scavenging HOCl molecules [118]. Quantum dot-silica monolith (QD-SM) with exchanged surface ligands of 6-mercaptohexanol (6-MHOH) was much stabile than the QD-SM prepared with 3-mercaptopropyltrimethoxysilane (3-MPS), since the 6-MHOH can effectively resist against the oxidative damage to the ZnS shell caused by hydroxide ions [45].

QDs with core/polymer shell structure provide unique combination of enhanced dispersity as well as photostability after the mixture with the polymer matrix. Metal core coated with polymers, such as polyaniline, polypyrole, and polythiophene, have attracted
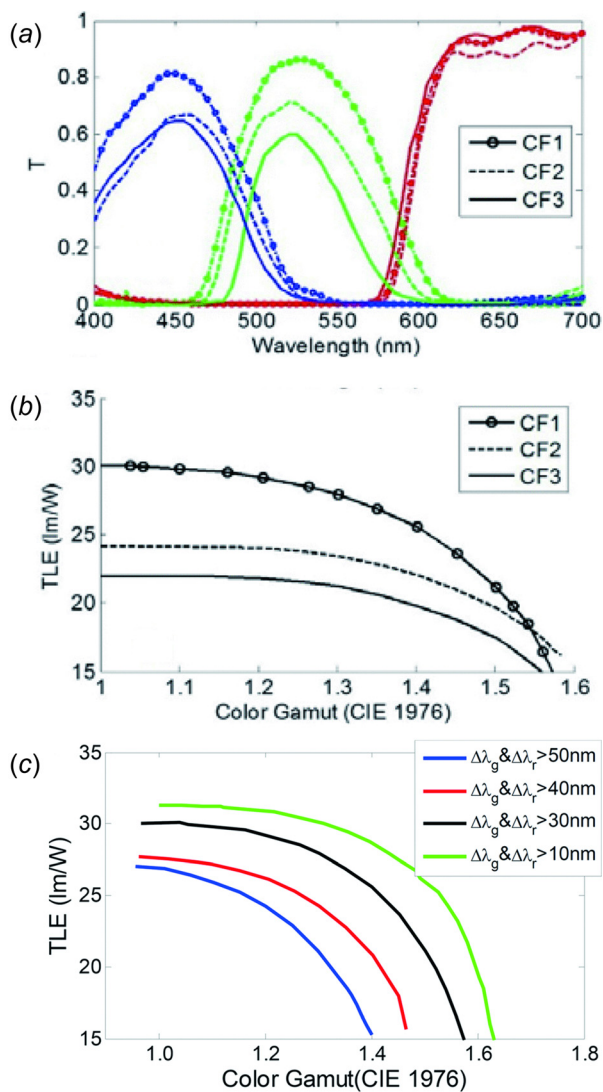
much interest for use in light-emitting devices [118–120]. Nevertheless, these polymers can hardly be commercialized because of its poor processability. Many groups have developed the QDs/PMMA nanocomposites [121–124]; PMMA was suitable due to its optical transparency; and the PMMA shell also plays a role in protecting the surface of QDs core from oxidation. In addition, there is also no significant loss in quantum yield (~12% to ~8%) after polymer coating.

Fig. 14 (*a*) Cross-sectional SEM images of one side of the QDs plate dip-coated with hybrid layers of PVP/silica. Variation of the (*b*) EL spectra and (*c*) luminous efficacy and light conversion efficiency of the QDs plate-based WLED with increasing forward current. The insets in (*a*) show the device schematic and photographs of the remote-type, resin-free QD-LEDs operating at 20 mA and 300 mA. (*d*) Temporal evolution of the EL spectra of the QD-LEDs operated at 20 mA for a prolonged duration up to 20 h [129].

Compared with the overcoat layer on the surface of nanocrystals, an extra barrier layer on the surface of QDs–polymer hybrid film is easier to be processed for realizing a QDs–polymer film against photo-oxidation. A single inorganic barrier layer generated by a vacuum processing provided an enhancement of two or three orders of magnitude over OTR for polymeric substrates [125]. Analogy to OLED packaging, barrier layers which are impermeable to oxygen and moisture, such as SiO_x [125–127], SiN_x [127], and Al_2O_3 [128], have been utilized to form high gas-resistant substrates. To acquire a high coating quality of the barrier layer, the wetting compatibility between the polymer matrix and the barrier should be examined. For instance, Fig. 14 shows a direct dip coating of the QDs–PMMA hybrid film into silica sol, which results in a poor compatibility. And a polyvinylpyrrolidone (PVP) was suitable as an interfacial adhesion layer for ensuring uniform deposition of the subsequent silica barrier layer [129].
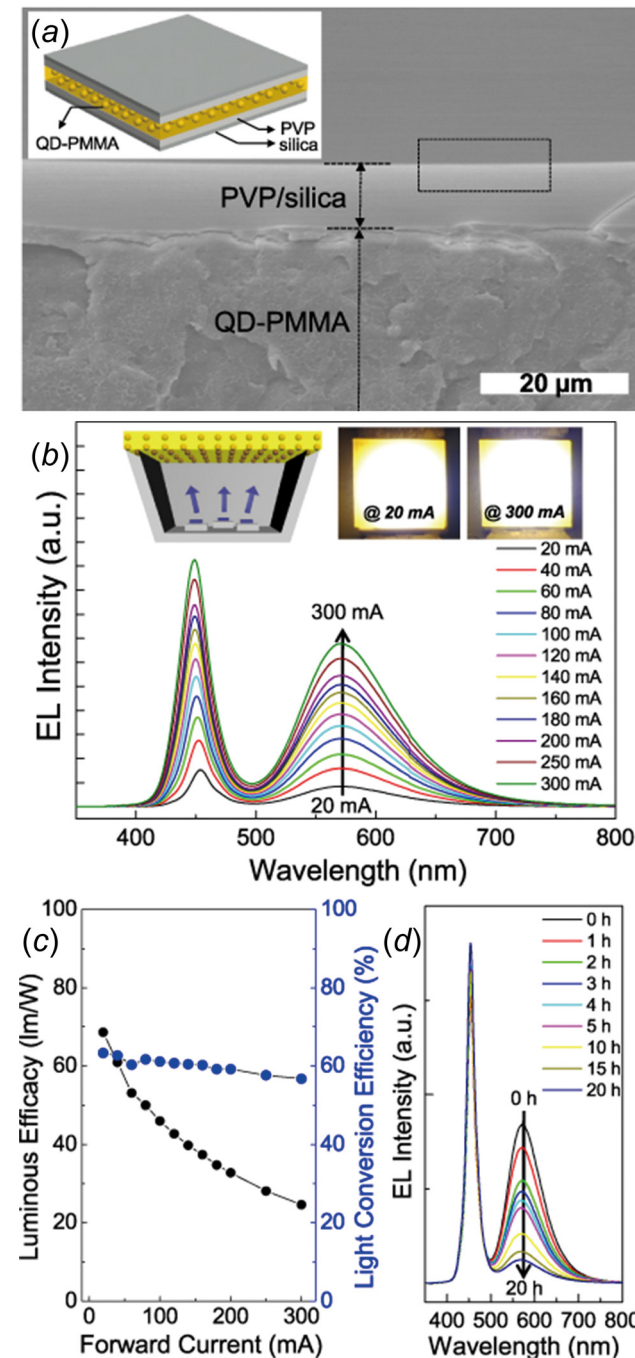
4.3.2 Enhancing the Thermal Stability of QD-LEDs. It was concluded from previous researches that the PL intensity of QDs decreased as the temperature increased [112,130]. Therefore, to optimize the packaging structure of QD-LEDs and consequently lower the working temperature of QDs is of importance. In our previous work, we compared the optical and thermal performances of three different packaging structures: air encapsulation (type 1), silicone lens (type 2), and silicone encapsulation (type 3) [131]. Figures 15(*a*) and 15(*b*) plot the schematic diagrams and photographs of these three packages: in type 1, the inner space between QDs–polymer film and LED chip is filled with air; in the type 2, a silicone lens is coated on the LED chip; while in type 3, silicone gel is filled into the space between QDs–polymer film and LED chip. CdSSe/ZnS core–shell QDs with WL = 574 nm were mixed with PMMA to fabricate the QDs–polymer film. Figure 15(*c*) plots the temperature fields of three packages under driving current of 300 mA. It is seen from the experiment data that the maximum temperature of QDs–polymer film in type 1, 2, and 3 are 110.7 °C, 112.0 °C, and 85.4 °C, respectively. Due to the lower QDs temperature in type 3 than those of in type 1 and 2, when the driving current increased from 50 mA to 500 mA, the QDs peak emission of type 1 dropped by 36.8% and type 2 dropped by 20.4%, while that of type 3 only dropped by 6.2%, as shown in Fig. 15(*d*). Therefore, polymer encapsulation plays an important role in stabilizing the QDs' performance.

In addition to the polymer encapsulation structure, the configuration of QDs layer also influences the thermal stability performance of QD-LEDs. Yin et al. studied the thermal performances of the CRI for two types of QD-LEDs [132]. It was found that QD-LEDs with the encapsulation of yellow phosphors and red QDs exhibited higher CRI and lower sensitivity to the temperature than those with the encapsulation of yellow and red phosphors. When the ambient temperature increased from 25 °C to 100 °C, the CRI of QD-LEDs with yellow phosphor and red QDs changed only 0.3, while that with yellow and red phosphor changed 2.2. Since the heat generation of QDs–polymer layer was derived from the optical loss, enhancing the light output efficiency of QDs layer can also enhance the thermal reliability of QD-LEDs. Han et al. studied the effect of three different composite structures (QDs on phosphor, phosphor on QDs, and mixed) on the optical and thermal characteristics [133]. It was found that the layered structure is more effective than the mixed one with respect to PL intensity, PL decay, and thermal loss. When the QDs on phosphor-layered nanocomposite are used to fabricate a QD-LEDs, the brightness was increased by 37%, and the CRI was raised to 88.4 compared to that of mixed case of 80.4%. Figure 16 plots the schematic diagram of the energy transfer between QDs and phosphor. For the QDs layer on the phosphor structure (Fig. 16(*a*)), most of the blue light is first converted by phosphor with high efficiency, and then, QDs are used to convert the blue light and the green light from the phosphor. However, for the phosphor on QDs layer structure (Fig. 16(*b*)), if the QDs absorb most of the blue light, they emit the converted red light at a low conversion efficiency. Therefore, it is
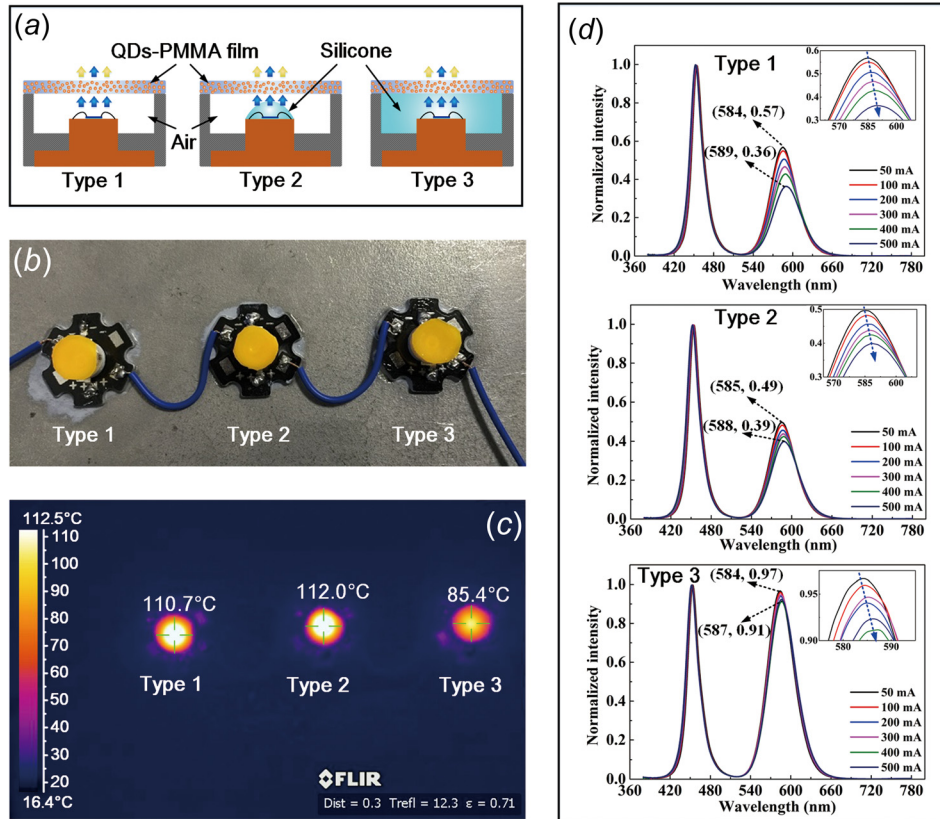
Fig. 15 (*a*) Schematic diagrams of three different QD-LEDs packaging structures. (*b*) Image of three QD-LEDs packages. (*c*) Temperature fields of three QD-LEDs packages measured by infrared thermal imager under driving current of 300 mA. (*d*) Normalized emission spectra of three types of QD-LEDs packages at varying driving current. The inset in each figure shows the corresponding details of QDs emission peak [131].

better to place the QDs on the outer layer rather than the layer near the light source. For the mixed layer (Fig. 16(*c*)), energy transfer and energy loss occurred simultaneously. Consequently, the emission loss is expected to increase due to the increased optical interface between the QDs and phosphor [133].

Other strategies to enhance the light output efficiency have been proposed as well. Oh et al. introduced microlens and microprism to the front side of QD-LEDs to enhance the extraction efficiency [134]. The microlens-attached QD-LEDs have a high luminescence values, which was 1.57 times higher than those of conventional QD-LEDs. Shin et al. proposed an air-gap structure to enhance the optical extraction efficiency of QD-LEDs [135]. The proposed structure showed enhancement of 29.7% by

experiment as compared with that of a remote layer-by-layer QDs' structure without an air gap. This was attributed to the fact that some re-emitted and scattered light from QDs can be reflected again by total internal reflection at the interface between the QDs–polymer layer and air to reduce the absorption loss in the package.

5 Summary and Perspectives

Quantum dots light-emitting diodes have developed tremendously over the past two decades, and progress has been especially fast recently due to significant improvements in the quality of QDs materials as well as advances in the packaging strategies
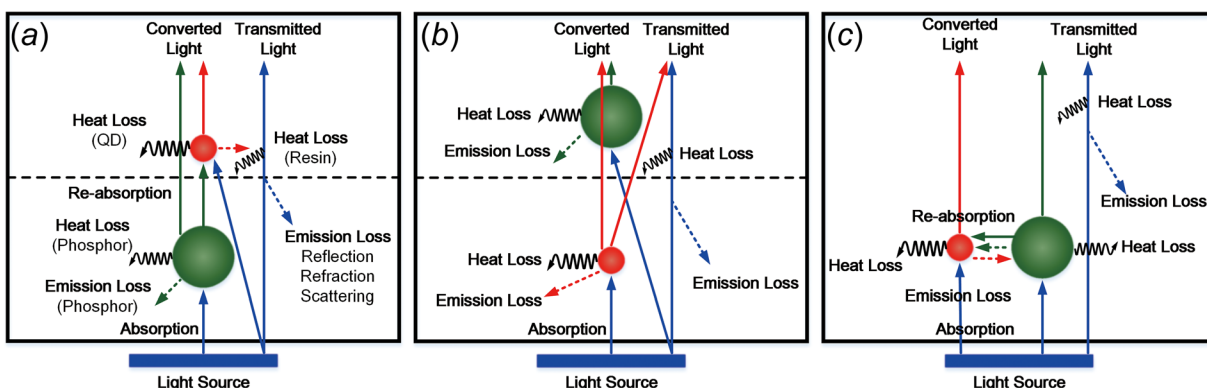

Fig. 16 Schematic illustration of the emission mechanism and the energy transfer between QDs and phosphor in polymer matrix: (*a*) QDs layer on phosphor layer, (*b*) phosphor layer on QDs layer, and (*c*) mixed layer [133]

of the devices. In this review, we introduced the applications of QDs-LEDs in the lighting and display industries, and then, the challenges in QD-LEDs packaging and the progresses were overviewed. With the objective of developing QD-LEDs with high efficiency, color-rendering ability, and stability, researchers have devoted to solve the packaging problems, such as the incompatibility of QDs with polymer matrix when fabricating QDs–polymer film, the spectra optimization of QD-LEDs by both simulation and experiments, and the stability enhancement of QD-LEDs against penetrative oxygen and moisture as well as the high temperature.

It is noted here that we only reviewed the packaging strategies of QD-LEDs in this work, while the intrinsic properties of the as-prepared QDs are as important as the packaging. That is, the synthesis of QDs materials should be well investigated to ensure the high quantum yields and stability of QDs. Specially, due to the toxicity of cadmium element toward human body, new QDs materials with cadmium-free, high quantum yields and full spectrum are badly needed. From the research hotspots in QDs synthesis, I–III–VI group of QDs and all-inorganic perovskite QDs are expected to be the alternatives of cadmium-based QDs after the improvements of their stability and spectrum tenability. Status of this research area can be found in the review by Vasudevan et al. [136] and Hines et al. [137].

It should be pointed out that most of the achievements for high-performance QD-LEDs are built upon experimental trial and error. In the coming decade, more fundamental researches about optical properties of QD-LEDs have to be carried out to better understand the mechanisms of QD-LEDs' energy propagation and conversion. Light absorption, scattering, and converting behaviors in QDs–polymer composites need to be observed to provide a theoretical guidance on experimental design. Only at that point, we will have a scientific basis for packaging QD-LEDs with specific photonic properties.

Besides, the heat generation inside of the QD-LEDs package needs to be predicted via thermal modeling, thus the thermal performances of different packaging structure can be evaluated and optimized. Moreover, it has been concluded that the thermal conductivity of QDs layer was orders of magnitude lower than that of traditional semiconductors [138]. Therefore, thermal conductivity of QDs–polymer layer needs to be reinforced to improve stability and efficiency of the whole QD-LEDs package. In addition, with the development of large-size LCD display, searching for new packaging strategies for the fabrication of large-scale, high-uniformity QD-LEDs module is a promising direction toward promoting industrialization of QD-LEDs products.

Acknowledgment

References

[1] Kwak, J., Bae, W. K., Lee, D., Park, I., Lim, J., Park, M., Cho, H., Woo, H., Yoon, D. Y., and Char, K., 2012, "Bright and Efficient Full-Color Colloidal Quantum Dot Light-Emitting Diodes Using an Inverted Device Structure," Nano Lett., 12(5), pp. 2362–2366.

[2] Cho, J. S., Lee, E. K., Joo, W. J., Jang, E., Kim, T. H., Lee, S. J., Kwon, S. J., Han, J. Y., Kim, B. K., and Choi, B. L., 2009, "High-Performance Crosslinked Colloidal Quantum-Dot Light-Emitting Diodes," Nat. Photon., 3(6), pp. 341–345.

[3] Zhang, Y., Xie, C., Su, H., Liu, J., Pickering, S., Wang, Y., Yu, W., Wang, J., Wang, Y., and Hahm, J.-I., 2011, "Employing Heavy Metal-Free Colloidal Quantum Dots in Solution-Processed White Light-Emitting Diodes," Nano Lett., 11(2), pp. 329–332.

[4] Xie, R., Kolb, U., Li, J., Basche, T., and Mews, A., 2005, "Synthesis and Characterization of Highly Luminescent CdSe-Core CdS/Zn$_{0.5}$Cd$_{0.5}$S/ZnS Multishell Nanocrystals," J. Am. Chem. Soc., 127(20), pp. 7480–7488.

[5] Yang, X., Zhao, D., Leck, K. S., Tan, S. T., Tang, Y. X., Zhao, J., Demir, H. V., and Sun, X., 2012, "Full Visible Range Covering InP/ZnS Nanocrystals With High Photometric Performance and Their Application to White Quantum Dot Light-Emitting Diodes," Adv. Mater., 24(30), pp. 4180–4185.

[6] Kim, J.-H., and Yang, H., 2014, "All-Solution-Processed, Multilayered CuInS$_2$/ZnS Colloidal Quantum-Dot-Based Electroluminescent Device," Opt. Lett., 39(17), pp. 5002–5005.

[7] Bruchez, M., Moronne, M., Gin, P., Weiss, S., and Alivisatos, A. P., 1998, "Semiconductor Nanocrystals as Fluorescent Biological Labels," Science, 281(5385), pp. 2013–2016.

[8] Huynh, W. U., Dittmet, J. J., and Alivisatos, A. P., 2002, "Hybrid Nanorod-Polymer Solar Cells," Science, 295(5564), pp. 2425–2427.

[9] Lee, J., Sundar, V. C., Heine, J. R., Bawendi, M. G., and Jensen, K. F., 2000, "Full Color Emission From II–VI Semiconductor Quantum Dot-Polymer Composites," Adv. Mater., 12(15), pp. 1102–1105.

[10] Coe, S., Woo, W. K., Bawendi, M., and Bulovic, V., 2002, "Electroluminescence From Single Monolayers of Nanocrystals in Molecular Organic Devices," Nature, 420(6917), pp. 800–803.

[11] Lall, P., and Zhang, H., 2015, "Assessment of Lumen Degradation and Remaining Life of Light-Emitting Diodes Using Physics-Based Indicators and Particle Filter," ASME J. Electron. Packag., 137(2), p. 021002.

[12] Petroski, J., 2014, "Advanced Natural Convection Cooling Designs for Light-Emitting Diode Bulb Systems," ASME J. Electron. Packag., 136(4), p. 041007.

[13] Liu, Z., Liu, S., Wang, K., and Luo, X., 2010, "Measurement and Numerical Studies of Optical Properties of YAG:Ce Phosphor for White Light-Emitting Diode Packaging," Appl. Opt., 49(2), pp. 247–257.

[14] Lin, C. C., and Liu, R.-S., 2011, "Advances in Phosphors for Light-Emitting Diodes," J. Phys. Chem. Lett., 2(11), pp. 1268–1277.

[15] Wang, X., Zhou, G., Zhang, H., Li, H., Zhang, Z., and Sun, Z., 2012, "Luminescent Properties of Yellowish Orange Y$_3$Al$_{5-x}$Si$_x$O$_{12-x}$N$_x$:Ce Phosphors and Their Applications in Warm White Light-Emitting Diodes," J. Alloy. Compd., 519, pp. 149–155.

[16] Cho, J., Kim, H., Sone, C., Park, Y., Kim, Y. S., Kubota, S., and Yoon, E., 2009, "Study of UV Excited White Light-Emitting Diodes for Optimization of Luminous Efficiency and Color Rendering Index," Phys. Status. Solidi-R., 3(1), pp. 34–36.

[17] Li, X., Wu, Y., Zhang, S., Cai, B., Gu, Y., Song, J., and Zeng, H., 2016, "CsPbX$_3$ Quantum Dots for Lighting and Displays: Room-Temperature Synthesis, Photoluminescence Superiorities, Underlying Origins and White Light-Emitting Diodes," Adv. Funct. Mater. (in press).

[18] Kim, T.-H., Jun, S., Cho, K. S., Chio, B. L., and Jang, E., 2013, "Bright and Stable Quantum Dots and Their Applications in Full-Color Displays," MRS Bull., 38(9), pp. 712–720.

[19] Schubert, E. F., and Kim, J. K., 2005, "Solid-State Light Sources Getting Smart," Science, 308(5726), pp. 1274–1278.

[20] Schubert, E. F., Kim, J. K., Luo, H., and Xi, J.-Q., 2006, "Solid-State Lighting—A Benevolent Technology," Rep. Prog. Phys., 69(12), pp. 3069–3099.

[21] Shirasaki, Y., Supran, G. J., Bawendi, M. G., and Bulovic, V., 2013, "Emergence of Colloidal Quantum-Dot Light-Emitting Technologies," Nat. Photonics, 7(1), pp. 13–23.

[22] Talapin, D. V., and Steckel, J., 2013, "Quantum Dot Light-Emitting Devices," MRS Bull., 38(9), pp. 685–695.

[23] Unnithan, A. R., Barakat, N. A. M., Abadir, M. F., Yousef, A., and Kim, H. Y., 2012, "Novel CdPdS/PVAc Core-Shell Nanofibers as an Effective Photo-catalyst for Organic Pollutants Degradation," J. Mol. Catal. A: Chem., 363–364, pp. 186–194.

[24] Wu, Y., Bao, B., Su, B., and Jiang, L., 2013, "Directed Growth of Calcein/Nile Red Coaxial Nanowire Arrays Via a Two-Step Dip-Coating Approach," J. Mater. Chem. A, 1(30), pp. 8581–8586.

[25] Kakati, J., and Datta, P., 2013, "On Characteristics of PVA/CdS and PVA/CdS:Cu Nanocomposites for Applications as LED," J. Lumin., 138, pp. 25–31.

[26] Kharazmi, A., Saion, E., Faraji, N., Soltani, N., and Dehzangi, A., 2013, "Optical Properties of CdS/PVA Nanocomposite Films Synthesized Using the Gamma-Irradiation-Induced Method," Chinese Phys. Lett., 30(5), p. 057803.

[27] Li, Y., Zhang, W., Li, K., Yao, Y., Niu, J., and Chen, Y., 2012, "Oxidative Dissolution of Polymer-Coated CdSe/ZnS Quantum Dots Under UV Irradiation: Mechanisms and Kinetics," Environ. Pollut., 164, pp. 259–266.

[28] Fragoulu, D., Resta, V., Pompa, P. P., Laera, A. M., Gaputo, G., Tapfer, L., Cingolani, R., and Athanassiou, A., 2009, "Patterned Structures of In Situ Size Controlled CdS Nanocrystals in a Polymer Matrix Under UV Irradiation," Nanotechnology, 20(15), p. 155302.

[29] Chu, M., Zhou, L., Song, X., Pan, M., Zhang, L., Sun, Y., Zhu, J., and Ding, Z., 2006, "Incorporating Quantum Dots Into Polymer Microspheres Via a Spray-Drying and Thermal Denaturizing Approach," Nanotechnology, 17(6), pp. 1791–1796.

[30] Sato, M., Kawata, A., Morito, S., Sato, Y., and Yamaguchi, I., 2008, "Preparation and Properties of Polymer/Zinc Oxide Nanocomposites Using Functionalized Zinc Oxide Quantum Dots," Eur. Polym. J., 44(11), pp. 3430–3438.

[31] Yoon, C., Hong, H.-G., Kim, H. C., Hwang, D., Lee, D. C., Kim, C. K., Kim, Y. J., and Lee, K., 2013, "High Luminescence Efficiency White Light Emitting Diodes Based on Surface Functionalized Quantum Dots Dispersed in Polymer Matrices," Colloid Surf. A, 428, pp. 86–91.

[32] Kim, H., Jang, H. S., Kwon, B.-H., Suh, M., Kim, Y., Cheong, S. H., and Jeon, D. Y., 2012, "In Situ Synthesis of Thiol-Capped CuInS$_2$-ZnS Quantum Dots

[33] Qu, H., Cao, L., Su, G., and Liu, J., 2013, "Effect of Inorganic Shells on Luminescence Properties of ZnS:Ag Nanoparticles," J. Mater. Sci., 48(14), pp. 4952–4961.

[34] Reitinger, N., Hohenau, A., Kostler, S., Krenn, J. R., and Leitner, A., 2011, "Radiationless Energy Transfer in CdSe-ZnS Quantum Dot Aggregates Embedded in PMMA," Phys. Status Solidi A, 208(3), pp. 710–714.

[35] Wang, X., Li, W., and Sun, K., 2011, "Stable Efficient CdSe/CdS/ZnS Core/Multi-Shell Nanophosphors Fabricated Through a Phosphine-Free Route for White Light-Emitting-Diodes With High Color Rendering Properties," J. Mater. Chem., 21(24), pp. 8558–8565.

[36] Mamedov, A. A., Belov, A., Giersig, M., Mamedova, N. N., and Kotov, N. A., 2001, "Nanorainbows: Graded Semiconductor Films From Quantum Dots," J. Am. Chem. Soc., 123(31), pp. 7738–7739.

[37] Gao, M., Sun, J., Dulteith, E., Gaponik, N., Lemmer, U., and Feldmann, J., 2002, "Lateral Patterning of CdTe Nanocrystal Films by the Electric Field Directed Layer-by-Layer Assembly Method," Langmuir, 18(10), pp. 4098–4102.

[38] Murakoshi, K., Hosokawa, H., Saito, M., Wada, Y., and Yanagida, S., 1998, "Control of Surface Coverage and Solubility of Thiophenolate-Capped CdS Nanocrystallites," J. Colloid Interface Sci., 203(1), pp. 225–228.

[39] Tamborra, M., Striccoli, M., Comparelli, R., Curri, M. L., Petrella, A., and Agostiano, A., 2004, "Optical Properties of Hybrid Composites Based on Highly Luminescent CdS Nanocrystals in Polymer," Nanotechnology, 15(4), pp. S240–S244.

[40] Erskine, L. L., Emrick, T., Alivisatos, A. P., and Frechet, J. M. J., 2000, "Preparations of Semiconductor Nanocrystal-Polystyrene Hybrid Materials," Spring National Americal Chemical Society Meeting, San Francisco, CA, Mar. 26–31.

[41] Zhang, H., Cui, Z., Wang, Y., Zhang, K., Ji, X., Lu, C., Yang, B., and Gao, M., 2003, "From Water-Soluble CdTe Nanocrystals to Fluorescent Nanocrystal-Polymer Transparent Composites Using Polymerizable Surfactants," Adv. Mater., 15(10), pp. 777–780.

[42] Zhao, B., Yao, X., Gao, M., Sun, K., Zhang, J., and Li, W., "Doped Quantum Dots@Silica Nanocomposites for White Light-Emitting Diodes," Nanoscale, 7(41), pp. 17231–17236.

[43] Yang, P., Ando, M., and Murase, N., 2011, "Highly Luminescent CdSe/Cd_xZn_{1−x}S Quantum Dots Coated With Thickness-Controlled SiO_2 Shell through Silanization," Langmuir, 27(15), pp. 9535–9540.

[44] Zhou, C., Shen, H., Wang, H., Xu, W., Mao, M., Wang, S., and Li, L. S., 2012, "Synthesis of Silica Protected Photoluminescence QDs and Their Applications for Transparent Fluorescent Films With Enhanced Photochemical Stability," Nanotechnology, 23(42), p. 425601.

[45] Kim, H., Jang, H. S., Kwon, B. H., Suh, M., Kim, Y., Cheong, S. H., and Jeon, D. Y., 2012, "In Situ Synthesis of Thiol-Capped CuInS_2-ZnS Quantum Dots Embedded in Silica Powder by Sequential Ligand-Exchange and Silanization," Electrochem. Solid-State Lett., 15(2), pp. K16–K18.

[46] Kim, Y.-K., Chio, K.-C., Ahn, S.-H., and Cho, Y.-S., 2012, "A Facile Synthesis of SiO_2-Based Nanocomposites Containing Multiple Quantum Dots at High Concentration for LED Applications," RSC Adv., 2(16), pp. 6411–6413.

[47] Woo, H., Lim, J., Lee, Y., Sung, J., Shin, H., Oh, J. M., Chio, M., Yoon, H., Bae, W. K., and Char, K., 2013, "Robust, Processable, and Bright Quantum Dot/Organosilicate Hybrid Films With Uniform QD Distribution Based on Thiol-Containing Organosilicate Ligands," J. Mater. Chem. C, 1(10), pp. 1983–1989.

[48] Jun, S., Lee, J., and Jang, E., 2013, "Highly Luminescent and Photostable Quantum Dot-Silica Monolith and Its Application to Light-Emitting Diodes," ACS Nano, 7(2), pp. 1472–1477.

[49] Song, W.-S., Kim, J.-H., and Yang, H., 2013, "Silica-Embedded Quantum Dots as Downconverters of Light-Emitting Diode and Effect of Silica on Device Operational Stability," Mater. Lett., 111, pp. 104–107.

[50] Sun, H., Zhang, J., Zhang, H., Xuan, Y., Wang, C., Li, M., Tian, Y., Ning, Y., Ma, D., and Yang, B., 2006, "Pure White-Light Emission of Nanocrystal-Polymer Composites," Chemphyschem, 7(12), pp. 2492–2496.

[51] Zhang, H., Wang, C., Li, M., Ji, X., Zhang, J., and Yang, B., 2005, "Fluorescent Nanocrystal-Polymer Composites From Aqueous Nanocrystals: Methods Without Ligand Exchange," Chem. Mater., 17(19), pp. 4783–4788.

[52] Zhang, H., Wang, C., Li, M., Zhang, J., Lu, G., and Yang, B., 2005, "Fluorescent Nanocrystal-Polymer Complexes With Flexible Processability," Adv. Mater., 17(7), pp. 853–857.

[53] Tetsuka, H., Ebina, T., and Mizukami, F., 2008, "Highly Luminescent Flexible Quantum Dot-Clay Films," Adv. Mater., 20(16), pp. 3039–3043.

[54] Qi, W., Wang, Y., Yu, Z., Li, B., and Wu, L., 2013, "Fabrication of Transparent and Luminescent CdTe/TiO_2 Hybrid Film With Enhanced Photovoltaic Property," Mater. Lett., 107, pp. 60–63.

[55] Han, M., Gao, X., Su, J., and Nie, S., 2001, "Quantum-Dot-Tagged Microbeads for Multiplexed Optical Coding of Biomolecules," Nat. Biotechnol., 19(7), pp. 631–635.

[56] Chen, W., Wang, K., Hao, J., Wu, D., Wang, S., Qin, J., Li, C., and Cao, W., 2015, "Highly Efficient and Stable Luminescence From Microbeans Integrated With Cd-Free Quantum Dots for White-Light-Emitting Diodes," Part. Part. Syst. Charact., 32(10), pp. 922–927.

[57] Stsiapura, V., Sukhanova, A., Artemyev, M., Pluot, M., Cohen, J. H. M., Baranov, A. V., Oleinikov, V., and Nabiev, I., 2004, "Functionalized Nanocrystal-Tagged Fluorescent Polymer Beads: Synthesis, Physicochemical Characterization, and Immunolabeling Application," Anal. Biochem., 334(2), pp. 257–265.

[58] Bradley, M., Bruno, N., and Vincent, B., 2005, "Distribution of CdSe Quantum Dots Within Swollen Polystyrene Microgel Particles Using Confocal Microscopy," Langmuir, 21(7), pp. 2750–2753.

[59] Schubert, E. F., 2003, Light-Emitting Diodes, Cambridge University Press, Cambridge, UK, Chap. 12.

[60] Davis, W., and Ohno, Y., 2010, "Color Quality Scale," Opt. Eng., 49(3), p. 033602.

[61] Erdem, T., Nizamoglu, S., Sun, X., and Demir, H. V., 2010, "A Photometric Investigation of Ultra-Efficient LEDs With High Color Rendering Index and High Luminous Efficacy Employing Nanocrystal Quantum Dot Luminophores," Opt. Express, 18(1), pp. 340–347.

[62] Phillips, J. M., Coltrin, M. E., Crawford, M. H., Fischer, A. J., Krames, M. R., Mueller-Mach, R., Mueller, G. O., Ohno, Y., Rohwer, L. E. S., Simmons, J. A., and Tsao, J. Y., 2007, "Research Challenges to Ultra-Efficient Inorganic Solid-State Lighting," Laser Photonics Rev., 1(4), pp. 307–333.

[63] Zhong, P., He, G., and Zhang, M., 2012, "Optimal Spectra of White Light-Emitting Diodes Using Quantum Dot Nanophosphors," Opt. Express, 20(8), pp. 9122–9134.

[64] Chen, H.-S., Hsu, C.-K., and Hong, H.-Y., 2006, "InGaN–CdSe–ZnSe Quantum Dots White LEDs," IEEE Photonics Techol. Lett., 18(1–4), pp. 193–195.

[65] Chen, H.-S., Yeh, D.-M., Lu, C.-F., Huang, C.-F., Shiao, W.-Y., Huang, J.-J., Yang, C.-C., Liu, I.-S., and Su, W.-F., 2006, "White Light Generation With CdSe–ZnS Nanocrystals Coated on an InGaN-GaN Quantum-Well Blue/Green Two-Wavelength Light-Emitting Diode," IEEE Photonics Technol. Lett., 18(13–16), pp. 1430–1432.

[66] Nizamoglu, S., Ozel, T., Sari, E., and Demir, H. V., 2007, "White Light Generation Using CdSe/ZnS Core-Shell Nanocrystals Hybridized With InGaN/GaN Light Emitting Diodes," Nanotechnology, 18(6), p. 065709.

[67] Nizamoglu, S., Erdem, T., Sun, X., and Demir, H. V., 2010, "Warm-White Light-Emitting Diodes Integrated With Colloidal Quantum Dots for High Luminous Efficacy and Color Rendering," Opt. Lett., 35(20), pp. 3372–3374.

[68] Park, S. H., Hong, A., Kim, J. H., Yang, H., Lee, K., and Jang, H. S., 2015, "Highly Bright Yellow-Green-Emitting CuInS_2 Colloidal Quantum Dots With Core/Shell/Shell Architecture for White Light-Emitting Diodes," ACS Appl. Mater. Interfaces, 7(12), pp. 6764–6771.

[69] Song, W.-S., and Yang, H., 2012, "Fabrication of White Light-Emitting Diodes Based on Solvothermally Synthesized Copper Indium Sulfide Quantum Dots as Color Converters," Appl. Phys. Lett., 100(18), p. 183104.

[70] Kim, S., Kim, T., Kang, M., Kwak, S. K., Yoo, T. W., Park, L. S., Yang, I., Hwang, S., Lee, J. E., and Kim, S. K., 2012, "Highly Luminescent InP/GaP/ZnS Nanocrystals and Their Application to White Light-Emitting Diodes," J. Am. Chem. Soc., 134(8), pp. 3804–3809.

[71] Kim, K., Jeong, S., Woo, J. Y., and Han, C.-S., 2012, "Successive and Large-Scale Synthesis of InP/ZnS Quantum Dots in a Hybrid Reactor and Their Application to White LEDs," Nanotechnology, 23(6), p. 065602.

[72] Mutlugun, E., Hernandez-Martinez, P. L., Eroglu, C., Coskun, Y., Erdem, T., Sharma, V. K., Unal, E., Panda, S. K., Hickey, S. G., and Gaponik, N., 2012, "Large-Area (Over 50 cm × 50 cm) Freestanding Films of Colloidal InP/ZnS Quantum Dots," Nano Lett., 12(8), pp. 3986–3993.

[73] Gosnell, J. D., Schreuder, M. A., Rosenthal, S. J., and Weiss, S. M., 2007, "Efficiency Improvements of White-Light CdSe Nanocrystal-Based LEDs," Proc. SPIE, 6669, p. 66690R.

[74] Nizamoglu, S., and Demir, H. V., 2007, "Hybrid White Light Sources Based on Layer-by-Layer Assembly of Nanocrystals on Near-UV Emitting Diodes," Nanotechnology, 18(40), p. 405702.

[75] Ziegler, J., Xu, S., Kucur, E., Meister, F., Batentschuk, M., Gindele, F., and Nann, T., 2008, "Silica-Coated InP/ZnS Nanocrystals as Converter Material in White LEDs," Adv. Mater., 20(21), pp. 4068–4073.

[76] Shen, C., 2008, "CdSe/ZnS/CdS Core/Shell Quantum Dots for White LEDs," Proc. SPIE, 7138, p. 71382E.

[77] Wang, H., Lee, J.-S., Ryu, J.-H., Hong, C.-H., and Cho, Y.-H., 2008, "White Light Emitting Diodes Realized by Using an Active Packaging Method With CdSe/ZnS Quantum Dots Dispersed in Photosensitive Epoxy Resins," Nanotechnology, 19(14), p. 145202.

[78] Jang, H. S., Yang, H., Kim, S. W., Han, J. Y., Lee, S.-G., and Jeon, D. Y., 2008, "White Light-Emitting Diodes With Excellent Color Rendering Based on Organically Capped CdSe Quantum Dots and Sr_3SiO_5: Ce^{3+}, Li^+ Phosphors," Adv. Mater., 20(14), pp. 2696–2702.

[79] Jang, H. S., Kwon, B.-H., Yang, H., and Jeon, D. Y., 2009, "Bright Three-Band White Light Generated From CdSe/ZnSe Quantum Dot-Assisted Sr_3SiO_5:Ce^{3+},Li^+-Based White Light-Emitting Diode With High Color Rendering Index," App. Phys. Lett., 95(16), p. 161901.

[80] Yu, H. J., Park, K., Chung, W., Kim, J., and Kim, S. H., 2009, "White Light Emission From Blue InGaN LED Precoated With Conjugated Copolymer/Quantum Dots as Hybrid Phosphor," Synth. Met., 159(23–24), pp. 2474–2477.

[81] Song, W.-S., Kim, H.-J., Kim, Y.-S., and Yang, H., 2010, "Synthesis of Ba_2Si_3O_8:Eu^{2+} Phosphor for Fabrication of White Light-Emitting Diodes Assisted by ZnCdSe/ZnSe Quantum Dot," J. Electrochem. Soc., 157(10), pp. J319–J323.

[82] Gosnell, J. D., Rosenthal, S. J., and Weiss, S. M., 2010, "White Light Emission Characteristics of Polymer-Encapsulated CdSe Nanocrystal Films," IEEE Photonics Technol. Lett., 22(8), pp. 541–543.

[83] Dai, J., Ji, Z., Xu, C., Sun, X., Leck, K. S., and Ju, Z. G., 2011 "White Light Emission From CdTe Quantum Dots Decorated n-ZnO Nanorods/p-GaN Light-Emitting Diodes," Appl. Phys. Lett., 99(6), p. 063112.

[84] Chen, C., Chu, J., Qian, F., Zou, X., Zhong, C., Li, K., and Jin, S., 2012, "High Color Rendering Index White LED Based on Nano-YAG:Ce^{3+} Phosphor

Hybrid With CdSe/CdS/ZnS Core/Shell/Shell Quantum Dots," J. Mod. Opt., **59**(14), pp. 1199–1203.

[85] Zhu, L., Xu, L., Wang, J., Yang, S., Wang, C., Chen, L., and Chen, S., 2012, "Macromonomer-Induced CdTe Quantum Dots Toward Multicolor Fluorescent Patterns and White LEDs," RSC Adv., **2**(24), pp. 9005–9010.

[86] Song, W.-S., Kim, J.-H., Lee, J.-H., Do, Y. R., and Yang, H., 2012, "Synthesis of Color-Tunable Cu-In-Ga-S Solid Solution Quantum Dots With High Quantum Yields for Application to White Light-Emitting Diodes," J. Mater. Chem., **22**(41), pp. 21901–21908.

[87] Kwak, S. K., Yoo, T. W., Kim, B.-S., Lee, S. M., Lee, Y. S., and Park, L. S., 2012, "White LED Packaging With Layered Encapsulation of Quantum Dots and Optical Properties," Mol. Cryst. Liq. Cryst., **564**(1), pp. 33–41.

[88] Wang, R., Zhang, J., Xu, X., Wang, Y., Zhou, L., and Li, B., 2012, "White LED With High Color Rendering Index Based on Ca$_8$Mg(SiO$_4$)$_4$Cl$_2$:Eu^{2+} and ZnCdTe/CdSe Quantum Dot Hybrid Phosphor," Mater. Lett., **84**, pp. 24–26.

[89] Song, W.-S., Kim, J.-H., Lee, J.-H., Lee, H.-S., Jang, H. S., and Yang, H., 2013, "Utilization of LiSrPO$_4$:Eu Phosphor and Cu-In-S Quantum Dot for Fabrication of High Color Rendering White Light-Emitting Diode," Mater. Lett., **92**, pp. 325–329.

[90] Duan, H., Jiang, Y., Zhang, Y., Sun, D., Liu, C., Huang, J., Lan, X., Zhou, H., Chen, L., and Zhong, H., 2013, "High Quantum-Yield CdSe$_x$S$_{1-x}$/ZnS Core/Shell Quantum Dots for Warm White Light-Emitting Diodes With Good Color Rendering," Nanotechnology, **24**(28), p. 285201.

[91] Song, W.-S., Lee, S.-H., and Yang, H., 2013, "Fabrication of Warm, High CRI White LED Using Non-Cadmium Quantum Dots," Opt. Mater. Express, **3**(9), pp. 1468–1473.

[92] Yoon, H. C., Oh, J. H., and Do, Y. R., 2014, "High Color Rendering Index of Remote-Type White LEDs With Multi-Layered Quantum Dot-Phosphor Films and Short-Wavelength Pass Dichroic Filters," Proc. SPIE, **9190**, p. 919013.

[93] Liang, R., Yan, D., Tian, R., Yu, X., Shi, W., Li, C., Wei, M., Evans, D. G., and Duan, X., 2014, "Quantum Dots-Based Flexible Films and Their Application as the Phosphor in White Light-Emitting Diodes," Chem. Mater., **26**(8), pp. 2595–2600.

[94] Chuang, P.-H., Lin, C. C., and Liu, R.-S., 2014, "Emission-Tunable CuInS$_2$/ZnS Quantum Dots: Structure, Optical Properties, and Application in White Light-Emitting Diodes With High Color Rendering Index," ACS Appl. Mater. Interfaces, **6**(17), pp. 15379–15387.

[95] Jo, D.-Y., and Yang, H., 2015, "Spectral Broadening of Cu-In-Zn-S Quantum Dot Color Converters for High Color Rendering White Lighting Device," J. Lumin., **166**, pp. 227–232.

[96] Adam, M., Erdem, T., Stachowski, G. M., Soran-Erdem, Z., Lox, J. F. L., Bauer, C., Poppe, J., Demir, L. V., Gaponik, N., and Eychmuller, A., 2015, "Implementation of High-Quality Warm-White Light-Emitting Diodes by a Model-Experimental Feedback Approach Using Quantum Dot-Salt Mixed Crystals," ACS Appl. Mater. Interfaces, **7**(41), pp. 23364–23371.

[97] Li, F., Li, W., Fu, S., and Xiao, H., 2015, "Formulating CdSe Quantum Dots for White Light-Emitting Diodes With High Color Rendering Index," J. Alloy. Compd., **647**, pp. 837–843.

[98] Lin, H.-Y., Wang, S.-W., Lin, C.-C., Chen, K.-J., Han, H.-V., Tu, Z.-Y., Tu, H.-H., Chen, T.-M., Shih, M.-H., and Lee, P.-T., 2016, "Excellent Color Quality of White-Light-Emitting Diodes by Embedding Quantum Dots in Polymers Material," IEEE. J. Sel. Top. Quantum Electron., **22**(1), p. 2000107.

[99] QD Vision, 2013, "New Clor Technology Produces a TV Picture With the Most Radiant Reds, Brilliant Blues and Gorgeous Greens," QD Vision Inc., Lexington, MA, http://www.qdvision.com/content1566

[100] Nanosys, 2016, "QDEF: Quantum Dot Enhancement Film," Nanosys Inc., Milpitas, CA, http://www.nanosysinc.com/what-we-do/display-backlighting/qdef

[101] Coe-Sullivan, S., Liu, W., Allen, P., and Steckel, J. S., 2013, "Quantum Dots for LED Downconversion in Display Applications," ECS J. Solid State Sci. Technol., **2**(2), pp. R3026–R3030.

[102] Erdem, T., and Demir, H. V., 2013, "Color Science of Nanocrystal Quantum Dots for Lighting and Displays," Nanophotonics, **2**(1), pp. 57–81.

[103] Luo, Z., Chen, Y., and Wu, S.-T., 2013, "Wide Color Gamut LCD With a Quantum Dot Backlight," Opt. Express, **21**(22), pp. 26269–26284.

[104] Luo, Z., Xu, D., and Wu, S.-T., 2014, "Emerging Quantum-Dots-Enhanced LCDs," J. Disp. Technol., **10**(7), pp. 526–539.

[105] Zhu, R., Luo, Z., Chen, H., Dong, Y., and Wu, S.-T., 2015, "Realizing Rec. 2020 Color Gamut With Quantum Dot Displays," Opt. Express, **23**(18), pp. 23680–23693.

[106] Protesescu, L., Yakunin, S., Bodnarchuk, M. I., Krieg, F., Caputo, R., Hendon, C. H., Yang, R. X., Walsh, A., and Kivalenko, M. V., 2015, "Nanocrystals of Cesium Lead Halide Perovskites (CsPbX$_3$, X=Cl, Br, and I): Novel Optoelectronic Materials Showing Bright Emission With Wide Color Gamut," Nano Lett., **15**(6), pp. 3692–3696.

[107] Pathak, S., Sakai, N., Ricarola, F. W. R., Stranks, S. D., Liu, J., Eperon, G. E., Ducati, C., Wojciechowski, K., Griffiths, J. T., and Haghighirad, A. A., 2015, "Perovskite Crystals for Tunable White Light Emission," Chem. Mater., **27**(23), pp. 8066–8075.

[108] Mancini, M. C., Kairdolf, B. A., Smith, A. M., and Nie, S., 2008, "Oxidative Quenching and Degradation of Polymer-Encapsulated Quantum Dots: New Insights Into the Long-Term Fate and Toxicity of Nanocrystals In Vivo," J. Am. Chem. Soc., **130**(33), pp. 10836–10837.

[109] Buckner, S. W., Konold, R. L., and Jelliss, P. A., 2004, "Luminescence Quenching in PbS Nanoparticles," Chem. Phys. Lett., **394**(4–6), pp. 400–404.

[110] Tata, M., Banerjee, S., John, V. T., Waguespack, Y., and McPherson, G. L., 1997, "Fluorescence Quenching of CdS Nanocrystallites in AOT Water-in-Oil Microemulsions," Colloid Surf. A, **127**(1–3), pp. 39–46.

[111] Inerbaev, T. M., Masunov, A. E., Khondaker, S. I., Dobrinescu, A., and Plamada, A.-V., and Kawazoe, Y., 2009, "Quantum Chemistry of Quantum Dots-Effects of Ligands and Oxidation," J. Chem. Phys., **131**(4), p. 044106.

[112] Zhao, Y., Riemersma, C., Pietra, F., Koole, R., Donega, C. D., and Meijerink, A., 2012, "High-Temperature Luminescence Quenching of Colloidal Quantum Dots," ACS Nano, **6**(10), pp. 9058–9067.

[113] Chatterjee, S., and Mukherjee, T. K., 2015, "Thermal Luminescence Quenching of Amine-Functionalized Silicon Quantum Dots: A PH and Wavelength-Dependent Study," Phys. Chem. Phys. Chem., **17**(37), pp. 24078–24085.

[114] Cheng, T., Luo, X., Huang, S., and Liu, S., 2010, "Thermal Analysis and Optimization of Multiple LED Packaging Based on a General Analytical Solution," Int. J. Therm. Sci., **49**(1), pp. 196–201.

[115] Yuan, C., Li, L., Duan, B., Xie, B., Zhu, Y., and Luo, X., 2016, "Locally Reinforced Polymer-Based Composites for Efficient Heat Dissipation of Local Heat Source," Int. J. Therm. Sci., **102**, pp. 202–209.

[116] Yuan, C., Xie, B., Huang, M., Wu, R., and Luo, X., 2016, "Thermal Conductivity Enhancement of Platelets Aligned Composites With Volume Fraction From 10% to 20%," Int. J. Heat Mass Tran., **94**, pp. 20–28.

[117] Deng, Y., and Liu, J., 2010, "A Liquid Metal Cooling System for the Thermal Management of High Power LEDs," Int. Common. Heat. Mass., **37**(7), pp. 788–791.

[118] Guo, Z., Zhao, L., Pei, J., Zhou, Z., Gibson, G., Brug, J., Lam, S., and Mao, S. S., 2010, "CdSe/ZnS Nanoparticle Composites With Amine-Functionalized Polyfluorene Derivatives for Polymeric Light-Emitting Diodes: Synthesis, Photophysical Properties, and the Electroluminescent Performance," Macromolecules, **43**(4), pp. 1860–1866.

[119] Coe-Sullivan, S., Woo, W. K., Steckel, J. S., Bawendi, M., and Bulovic, V., 2003, "Tuning the Performance of Hybrid Organic/Inorganic Quantum Dot Light-Emitting Devices," Org. Electron., **4**(2–3), pp. 123–130.

[120] Smirnova, T. N., Sakhno, O. V., Yezhov, P. V., Kokhtych, L. M., Goldenberg, L. M., and Stumpe, J., 2009, "Amplified Spontaneous Emission in Polymer-CdSe/ZnS-Nanocrystal DFB Structures Produced by the Holographic Method," Nanotechnology, **20**(24), p. 245707.

[121] Jang, J., Kim, S., and Lee, K. J., 2007, "Fabrication of CdS/PMMA Core/Shell Nanoparticles by Dispersion Mediated Interfacial Polymerization," Chem. Commun., **26**, pp. 2689–2691.

[122] Khanna, R., Singh, N., Charan, S., Lonkar, S. P., Reddy, A. S., Patil, Y., and Viswanath, A. K., 2006, "The Processing of CdSe/Polymer Nanocomposites Via Solution Organometallic Chemistry," Mater. Chem. Phys., **97**(2–3), pp. 288–294.

[123] Song, H., and Lee, S., 2007, "Photoluminescent (CdSe) ZnS Quantum Dot-Polymethylmethacrylate Polymer Composite Thin Films in the Visible Spectral Range," Nanotechnology, **18**(5), p. 055402.

[124] Kwon, Y.-T., Choi, Y.-M., Kim, K.-H., Lee, C.-G., Lee, K.-J., Kim, B.-S., and Choa, Y.-H., 2014, "Synthesis of CdSe/ZnSe Quantum Dots Passivated With a Polymer for Oxidation Prevention," Surf. Coat. Technol., **259**(Part A), pp. 83–86.

[125] Lewis, J. S., and Weaver, M. S., 2004, "Thin-Film Permeation-Barrier Technology for Flexible Organic Light-Emitting Devices," IEEE J. Sel. Top. Quantum Electron., **10**(1), pp. 45–57.

[126] Iwamori, S., Gotoh, Y., and Moorthi, K., 2003, "Silicon Oxide Gas Barrier Films Deposited by Reactive Sputtering," Surf. Coat. Technol., **166**(1), pp. 24–30.

[127] Wuu, D.-S., Chen, T.-N., Wu, C.-C., Chiang, C.-C., Chen, Y.-P., Horng, R.-H., and Juang, F.-S., 2006, "Transparent Barrier Coatings for Flexible Organic Light-Emitting Diode Applications," Chem. Vap. Deposition, **12**(4), pp. 220–224.

[128] Meyer, J., Gorrn, P., Bertram, F., Hamwi, S., Winkler, T., Johnnes, H.-H., Weimann, T., Hinze, P., Riedl, T., and Kowalsky, W., 2009, "Al$_2$O$_3$/ZrO$_2$ Nanolaminates as Ultrahigh Gas-Diffusion Barriers—A Strategy for Reliable Encapsulation of Organic Electronics," Adv. Mater., **21**(18), pp. 1845–1849.

[129] Jang, E.-P., Song, W.-S., Lee, K.-H., and Yang, H., 2013, "Preparation of a Photo-Degradation-Resistant Quantum Dot-Polymer Composite Plate for Use in the Fabrication of a High-Stability White-Light-Emitting Diode," Nanotechnology, **24**(4), p. 045607.

[130] Shi, A., Wang, X., Meng, X., Liu, X., Li, H., and Zhao, J., 2012, "Temperature-Dependent Photoluminescence of CuInS$_2$ Quantum Dots," J. Lumin., **132**(7), pp. 1819–1823.

[131] Xie, B., Hu, R., Yu, X., Shang, B., Ma, Y., and Luo, X., 2016, "Effect of Packaging Method on Performance of Light-Emitting Diodes With Quantum Dot Phosphor," IEEE Photonics Technol. Lett., **28**(10), pp. 1115–1118.

[132] Yin, L., Bai, Y., Zhou, J., Cao, J., Sun, X., and Zhang, J., 2015, "The Thermal Stability Performances of the Color Rendering Index of White Light Emitting Diodes With the Red Quantum Dots Encapsulation," Opt. Mater., **42**, pp. 187–192.

[133] Woo, J. Y., Kim, K., Jeong, S., and Han, C.-S., 2011, "Enhanced Photoluminance of Layered Quantum Dot-Phosphor Nanocomposites as Converting Materials for Light Emitting Diodes," J. Phys. Chem. C, **115**(43), pp. 20945–20952.

[134] Oh, J. H., Choi, D. B., Lee, K.-H., Yang, H., and Do, Y. R., 2015, "Enhanced Light Extraction From Green Quantum Dot Light-Emitting Diodes by Attaching Microstructure Arrayed Films," IEEE J. Sel. Top. Quantum Electron, **22**(2), p. 2000206.

[135] Shin, M.-H., Hong, H.-G., Kim, H.-J., and Kim, Y.-J., 2014, "Enhancement of Optical Extraction Efficiency in White LED Package With Quantum Dot Phosphors and Air-Gap Structure," Appl. Phys. Express, **7**(5), p. 052101.

[136] Vasudevan, D., Gaddam, R. R., and Trinchi, A., 2015, "Core-Shell Quantum Dots: Properties and Applications," J. Alloy. Compd., **636**, pp. 395–404.

[137] Hines, D. A., and Kamat, P. V., 2014, "Recent Advances in Quantum Dot Surface Chemistry," ACS Appl. Mater. Interfaces, **6**(5), pp. 3041–3057.

[138] Ong, W.-L., Rupich, S. M., Talapin, D. V., McGaughey, A. J. H., and Malen, J. A., 2013, "Surface Chemistry Mediates Thermal Transport in Three-Dimensional Nanocrystal Arrays," Nat. Mater., **12**(5), pp. 410–415.